JPRS-JST-92-007
2 MARCH 1992

JPRS Report

Science & Technology

Japan:
Symposium on Applications of Advanced Technology: Sensors

Science & Technology

Japan

Symposium on Applications of Advanced Technology: Sensors

JPRS-JST-92-007 *2 March 1992*

CONTENTS

[Selected papers from FY91 Symposium on Applications of Advanced Technology: Sensors, held 3 Sep 91 in Nagoya, sponsored by the Japan Industrial Technology Association, Chubu Science and Technology Center, under the auspices of Chubu Bureau of International Trade and Industry, Government Industrial Research Institute, Nagoya, Agency of Industrial Science and Technology]

Symposium on Applications of Advanced Technology: Sensors

Table of Contents

Electrolytic Humidity Sensor Utilizing Solid Polymer Electrolytes

926C0010B Tokyo SENTAN GIJUTSU OYO SYMPOSIUM in Japanese 3 Sep 91 pp 1-4

[Article by A. Takenaka, Government Industrial Research Institute]

[Text]

1. Introduction

Since 1975, the author and his colleagues have been engaged in R&D on high efficiency hydrogen manufacturing by means of the water electrolysis of solid polymer electrolytes from the standpoint of developing energy-related technology. This method of water electrolysis is characteristic in that it employs a fluorinated resin cation film as a proton conductor, with the electrodes connected directly to the film, and through the technology development it demonstrates efficiency and productivity superior to those of the conventional method. At the same time, from the viewpoint of creating new electrochemical processes, we have been attempting to expand the developed technology to include electrochemical processes other than water electrolysis, such as hydrochloric acid electrolysis, the electrolysis of hydrobromic acid, ozone production and fuel cells that use solid polymer electrolytes.[1)]

The application of the technology to humidity sensors has been attempted as a part of a movement proposed by the author and his coworkers in 1983. In principle, it is a method that forcibly electrolyzes the moisture content supplied to the electrode in equilibrium with the humidity of the ambient atmosphere gas, and detects the humidity from the value of the current flowing at that time. The detection method is similar to that of the conventional phosphorus pentoxide sensor, and can be considered to come under the same category as the water electrolytic sensor. In contrast to the fact that the detection range of the phosphorus pentoxide sensor is limited to below several thousand parts per million because of its deliquiescence and cannot be used in an atmosphere of a gas which reacts with phosphorus pentoxide, the results of measurement of the characteristics of the proposed sensor revealed a wide detection range and excellent chemical stability, indicating its possible application as an inexpensive general purpose sensor. Here, we would like to summarize the characteristics of this unique humidity sensor, the element components, etc. Since the sensor is an electrolytic humidity sensor that makes use of a solid polymer electrolyte (SPE), it will be referred to as an SPE sensor in this article.

2. Constitution of Humidity-Sensitive Element

Figure 1 shows the constitution of the humidity-sensitive element. By using a film-electrode bonded body (a square several millimeters in size) obtained by directly bonding electrodes on both faces of a fluorinated resin cation film used as a solid polymer electrolyte, a fixed voltage greater than a voltage that shows the limiting current density is applied between the electrodes. The moisture content supplied to the electrodes from the ambient gas is forcibly electrolyzed according to the following equations:

$$\text{at the anode)}\ H_2O \rightarrow \tfrac{1}{2}\,O_2 + 2H^+ + 2e^- \quad (1)$$

$$\text{at the cathode)}\ 2H^+ + 2e^- \rightarrow H_2 \quad (2)$$

$$\text{total reaction)}\ H_2O \rightarrow H_2 + \tfrac{1}{2}\,O_2 \quad (3)$$

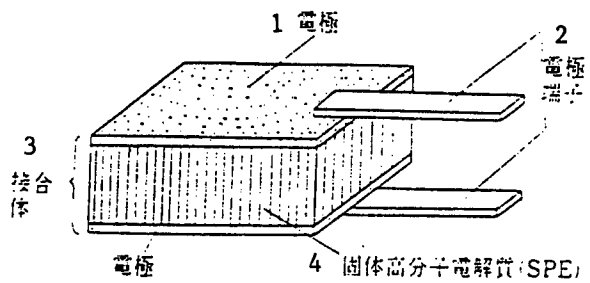

Figure 1. Humidity-Sensitive Element

Key: 1. Electrode 2. Electrode terminal 3. Bonded body 4. Solid polymer electrolyte (SPE)

The moisture content is electrolyzed at the anode and the protons generated pass through the film, generating hydrogen at the cathode. The current quantity at that time is exactly proportional to the quantity of moisture electrolyzed.

3. Component Materials

Just as in the electrolysis of water, a film which is a copolymer of tetrafluoroethylene and sulfonylfluoride vinyl ether and contains the sulfonic acid group, such as Nafion^{R} (made by DuPont), is appropriate as a fluorinated resin cation film to be used as an SPE. The electrode material to be bonded to such a film must be acid resistant, such as a platinum group metal, because the film is highly acidic. For bonding the electrode to the film, while available methods include thermocompression, which bonds an electrode sheet consisting of an electrode catalyst prepared in advance and a teflon binder, and a special chemical plating method developed by the author and his coworkers, the latter is capable of obtaining more satisfactory characteristics, as will be described later.

4. Sensor Characteristics

(1) Relationship between relative humidity and output current value Figure 2 shows the relationship between the output current density and the humidity for various kinds of bonded bodies with different kinds of electrodes, films (thickness and EW), and element sizes (0.01 to 0.25 cm^2). It can be seen that a satisfactory linear relationship can be obtained over a wide range of humidity for all elements.

Figure 3 shows the relationship between the applied voltage and the output current value for various relative humidities. When the applied voltage is raised beyond the theoretical decomposition voltage (1.23 V at 25°C) of water, the electrolysis of water starts, increasing the current and reaching the limiting current density in the vicinity of 3 V by having been rate determined by the supply of moisture from the ambient gas. With a further increase in voltage, a tendency for the current value to be reduced, especially on the high temperature side, is observed. Because of this, the influence of the set potential on the relationship between the relative humidity and the output current value is as shown in Figure 4. Although the tendency to deviate from the linear relationship on the high humidity side is seen for voltages exceeding 5 V, excellent linearity tends to occur on the low humidity side of less than 10 percent. Here, it is believed that the decrease in the current value on the high humidity side under high voltage is due not only to the reduction in the moisture supplied from the outside, but also to the increase in film resistance caused by the reduction in the water content of the film created by the electrolysis of part of the water contained in the film. The linear relationship shown in Figure 2 can be explained as follows.

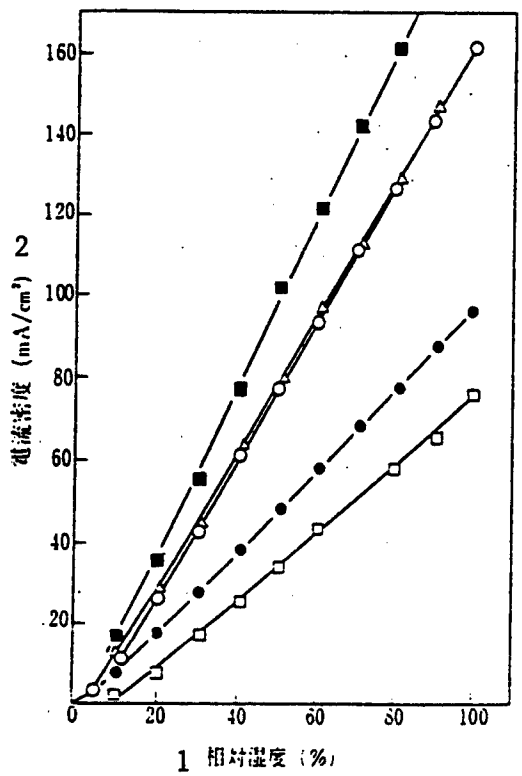

Figure 2. Relationship Between Relative Humidity and Current Density (at 300°C and 3.5 V) (Various marks in the figure represent different bonded bodies. The actual output current value for a bonded body of 0.1 cm^2, for example, is about 1/10.)

Key: 1. Relative humidity (%) 2. Current density (mA/cm^2)

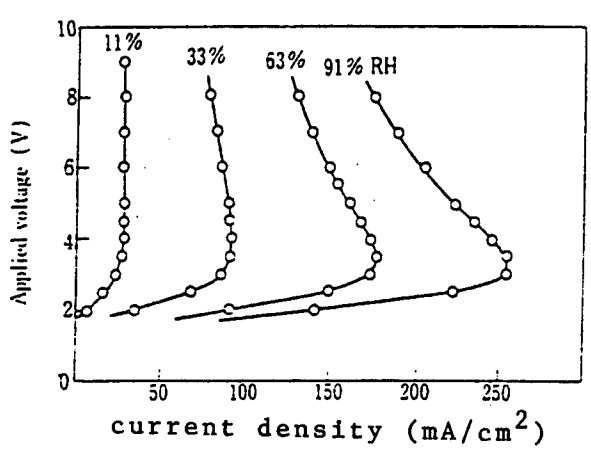

Figure 3. Relationship Between Applied Voltage and Current Density at Various Temperatures

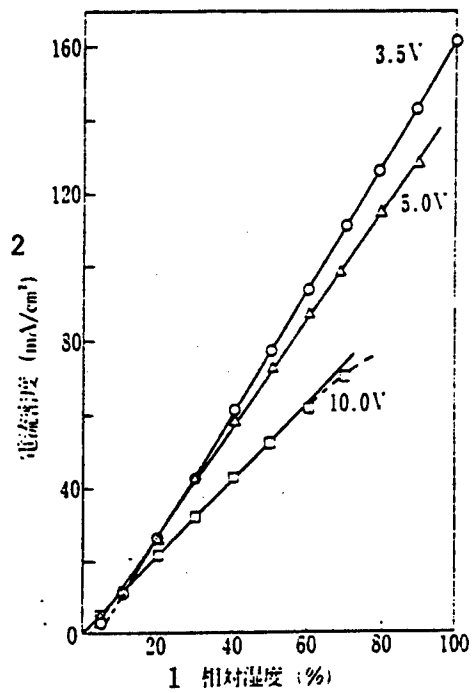

Figure 4. Relationship Between Relative Humidity and Current Density for Various Applied Voltages

Key: 1. Relative humidity (%) 2. Current density (mA/cm^2)

If the reaction rate is assumed to be determined by the supply of the moisture content to the anode, the flow speed of the moisture content can be represented by Fick's diffusion equation (4) below:

$$J_{H2O} = -D(dC_o/dx), \qquad (4)$$

where D is the diffusion coefficient, C_o the concentration of moisture content, and x the distance. If the thickness of the diffusion layer of δ and a linear distribution of the moisture content are assumed, one obtains:

$$J_{H2O} = -D[(C_o-C_s)/\delta] \qquad (5)$$

In the above equation, C_s is the concentration of the moisture content at the surface where the electrode reactions are actually taking place, and one obtains $C_s = 0$ for the limiting current density i_L. Since $i_L = 2FJ_{H2O}$, i_L can be approximated by the following equation:

$$i_L = 2FDC_o/\delta \qquad (6)$$

Therefore, i_L increases linearly with the increase in C_o. In other words, the fact that a linear relationship exists between the output current of an SPE sensor and the relative humidity is due to these reasons.

If it is assumed that the water electrolysis reaction takes place at the location where the electrolytic electrode, the electrode and the reaction substance are brought into mutual contact, then the reaction region will be limited to the neighborhood of the interface between the film and the electrode layer. Taking this into account, it is thought that the electrode layer outside the electrode bonded to the film acts as a diffused layer with uniform moisture content. Judging also from the experimental results that the output current is less for larger amounts of bonded metal and greater electrode layer thicknesses, and that the output current varies, even for the same amount of bonded metal, for different kinds of metals, leading to different precipitation conditions of the electrode layer, it can be seen that the electrode layer itself acts as a diffused layer. Therefore, the method used to bond the electrode to the film is extremely important, and the excellent linear relationship shown in Figure 2 cannot be obtained by mere thermocompression bonding using teflon, as mentioned above, or by the direct pressing of platinum pieces against the film.

(2) Response speed and stability

An example of the response speed of an SPE humidity sensor is shown in Figure 5. For changes from low to high humidity, the response speed for a rate of change of 90 percent was 2 to 3 minutes at 30°C and the time required to reach an equilibrium value was about 10 minutes. The response speed was higher for higher temperatures, with the corresponding times at 50°C about one-half those for the case at 30°C. For changes from high to low humidity, the response speed tended to be somewhat low. The hysteresis in the experiment shown in Figure 5 was within several percentage points.

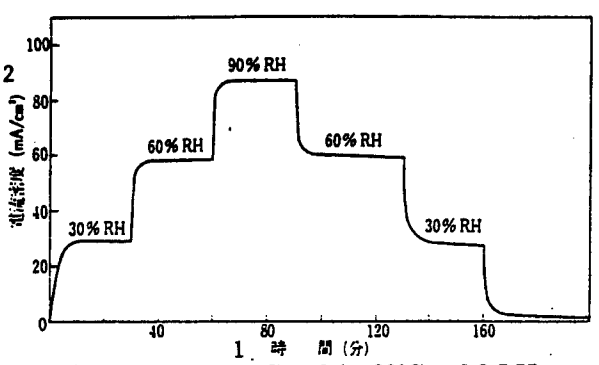

Figure 5. Response Speed (at 30°C and 3.5 V)

Key: 1. Time (minutes) 2. Current density (mA/cm^2)

The deterioration with time of the SPE humidity sensor varied somewhat for different bonded bodies, but for the case of bonding PtIr to Nafion^R 117 (2 mg/cm^2), in a test at 60 percent relative humidity and 27°C, the variation of the output current was within 5 percent at 50 days.

(3) Other factors affecting output current

The influence of the temperature on the output current is shown in Figure 6. For higher temperatures, the supplied moisture content is increased and hence the output current is increased. However, the plot of the output

current at various temperatures against the absolute temperature tends to decrease for higher temperatures, demonstrating a discrepancy with that given above.

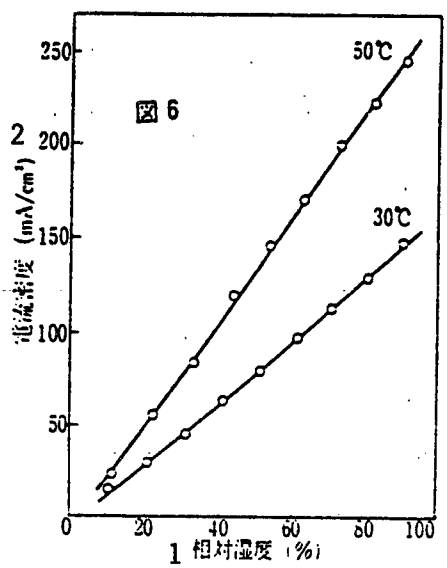

Figure 6.

Key: 1. Relative humidity (%) 2. Current density (mA/cm^2)

The output current is also affected by the flow speed of the ambient gas. For example, a change in gas speed from 0.2 to 2.0 cm/s at a constant humidity exhibits an increase in the output current of about 10 percent. However, since it is easy to avoid influencing the flow speed, the problem is believed to be minor for practical purposes.

The attachment of the electrode to the bonded body also affects the value of the output current. This is believed to be due to the difference in current distribution resutling from the electrical resistance of the electrode layer of the bonded body, the difference in the contact area between the electrode and the terminal, etc. It should be noted, however, that attempts to fix the terminals by means of fixing screws, springs or flat springs led to some changes in the absolute value of the output current, but to little change in the sensor characteristics.

5. Characteristics of SPE Humidity Sensor

From what has been said above, the characteristics that can be expected from the SPE humidity sensor can be summarized as follows:

(1) It has a satisfactory linear relationship, enabling measurements to be obtained over a wide range of humidity.

(2) Since the element material is stable chemically, as well as thermally, it has a long life and a wide range of usage.

(3) The element size can be minimized (0.01 to 0.04 cm^2), and mass production at a low cost is possible.

References

1. Takenaka, H., SODA AND CHLORINE, Vol 37, 1986 p 323.

2. NEWS OF THE GOVERNMENT INDUSTRIAL RESEARCH INSTITUTE, OSAKA, Vol 27 No 5, 1983 p 12; Takenaka, H., et al., SENSOR TECHNOLOGY, Vol 4, 1984 p 56.

Temperature Sensors for Low Temperatures (Rh-Fe Thermometers)

926C0010C Tokyo SENTAN GIJUTSU OYO SYMPOSIUM in Japanese 3 Sep 91 pp 15-19

[Article by Osamu Tamura, Metrology Laboratory, Agency of Industrial Science and Technology]

[Text]

1. Introduction

Accompanying the progress in recent years of such technologies as superconducting technology that employs low temperatures, the necessity for measuring low temperatures in various fields has been increasing. In addition, the accuracy of the absolute measurement of thermodynamic temperatures has been improved by the advancement of low temperature technology, with the measured data being expanded to still lower temperatures. Because of this, in January 1990 the 1968 International Practical Temperature Scales were revised to the 1990 International Temperature Scales (ITS-90)[1], with the defined lower limit temperature expanded from 13.81 K to 0.65 K. In this report, the temperature sensors used for maintenance and the revising of the temperature scales will be introduced, focusing on the expanded temperature range, and methods for improving these defects will be reported.

2. Resistance Temperature Sensors for Low Temperatures

Various kinds of resistance thermometers, capacitance thermometers and magnetic thermometers that utilize the temperature dependence of the electric resistivity, dielectric constant and magnetic permeability are being used as temperature sensors for low temperatures. Of these, resistance temperature sensors of platinum, platinum-cobalt (molar fraction 0.5 percent) and rhodium-iron (molar fraction of 0.5 percent) are in wide use for the maintenance and revision of the temperature scales for such reasons as their ease of handling, stability, reproducibility under the temperature cycle, and having a practical degree of sensitivity approaching room temperature. The temperature dependence of (dR/dt)/R, the relative sensitivity of the resistance R of the sensor according to temperature, is shown in Figure 1.

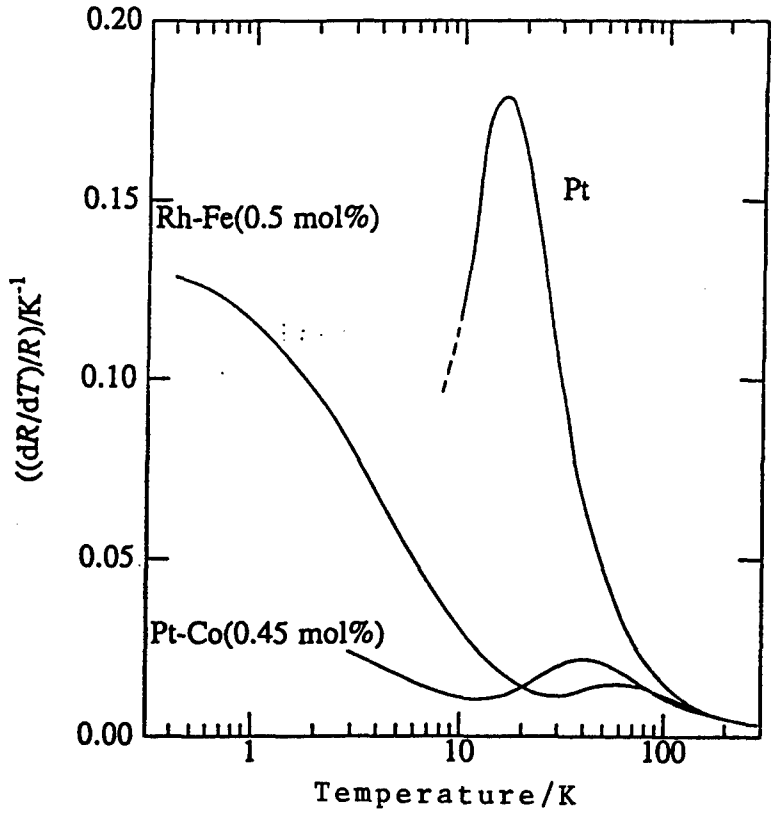

Figure 1. Temperature Characteristics of Relative Sensitivity of Resistance Temperature Sensors

Since the platinum temperature sensor is excellent with regard to sensitivity, stability and reproducibility over a wide temperature range, ITS-90 also employs it for temperature definition from about 14K to about 960°C. However, since its sensitivity deteriorates rapidly for temperatures below about 13K, the platinum-cobalt and rhodium-iron sensors are frequently used for lower temperatures. For temperatures below 20K, since the latter has greater sensitivity than the former, the rhodium-iron sensor is used most widely for maintaining and revising the scales in the field of precision measurement in this temperature region.

3. Improvement of Rhodium-Iron Temperature Sensor

3.1 Reduction of film thickness[4)]

As a result of the structure of the conventional rhodium-iron sensor, which is constructed so as to avoid having stress occur on the wire of the temperature-sensitive part as much as possible, its heat capacity is large and it is not easy to attain thermal equilibrium with the object of the temperature measurement at low temperatures. In particular, for temperatures below 1K, the helium gas sealed for heat exchange condenses, the thermal contact between the temperature-sensitive part and the object of temperature measurement deteriorates, and the measurement error is increased. In order to improve this defect, a sensor which has a rhodium-iron thin film as the temperature-sensitive part has been manufactured on a trial basis. If an insulator with relatively great heat conductivity at low temperatures is employed as the substrate, then it is possible to maintain the thermal contact between the temperature-sensitive part and the object of temperature measurement through solid conduction alone by adhering the rear surface of the substrate to the object of temperature measurement. Provided that temperature sensitivity comparable to that of a bulk material is obtainable at low temperatures, even if the film thickness is reduced, it can be used as a satisfactory temperature sensor with low heat capacity and a good thermal contact at low temperatures. A thin film with a thickness of several hundred nanometers was formed on a sapphire substrate by sputtering a rhodium-iron (molar fraction of 0.5 percent) target. The measured results of the temperature coefficient of the resistivity ρ of the thin film manufactured on a trial basis is shown in Figure 2. It can be seen from the figure that, even for a thin film, the sensitivity to temperature of the resistivity at low temperatures can be increased by mixing iron in rhodium, and that the thin film is effective as a temperature sensor.

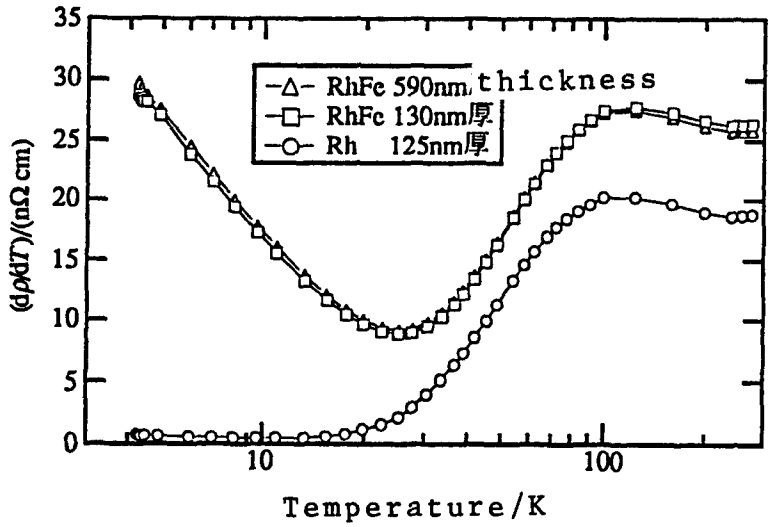

Figure 2. Sensitivity to Temperature of Electrical Resistivity of Rh-Fe and Rh Thin Films

3.2 Annealing of Wires[6]

In making a sensor by employing metallic or alloy wire as the temperature sensing part, it is recognized that annealing after winding the wire removes the strain generated in the wire during winding, significantly affecting the stability and reproducibility. As for rhodium-iron, the effect of annealing after winding the wire has been reported in the past only up to 750°C.[5] A temperature sensor using molten quartz as the reel for the rhodium-iron wire, making annealing at higher temperatures possible, has been devised and manufactured on a trial basis in order to investigate the annealing effect.

The structure of the trial-manufactured sensor is shown in Figure 3. First, a Rh-Fe (molar fraction of 0.5 percent) wire with a diameter of 0.05 mm was wound noninductively on a molten quartz reel with a cross-shaped cross section. After cleaning the sample with steam and annealing it in a helium gas atmosphere, the sample was housed in a platinum capsule, 45 mm long, with an outer diameter of 5 mm. For the purpose of heat exchange, helium gas of about 30 kPa was introduced to the capsule at room temperature, and the inter-conductor insulation and capsule sealing was carried out with lead glass.

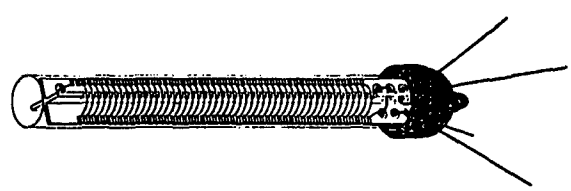

Figure 3. Rh-Fe Wire-Wound Temperature Sensor Using Molten Quartz Reel[6]

The annealing was conducted at 700, 800, 900 and 1,000°C. The results of measuring the change in resistance with the length of time during which the Rh-Fe wire is held at the specified temperatures are shown in Figure 4. The ordinate in the figure represents the ratio of the resistance measured at the triple point temperature of water to the resistance at the same temperature before annealing. The measurement was carried out by interrupting annealing at each point in time and lowering the temperature of the Rh-Fe wire. During the annealing at 1,000°C, the temperature was too high and the wire became brittle and could not be used as a sensor. For the case of temperatures from 700 to 900°C, the resistance was stabilized by annealing for about 1.5 hours. It can be said that that length of annealing is necessary.

The results of measuring the resistance-temperature characteristic at low temperatures using temperature sensors trial manufactured and annealed as reported above are shown in Figure 5. The ordinate in the figure represents $W = R/R_{tr}$, the ratio of the resistance R to the resistance R_{tr} at the triple point temperature of water. For purposes of comparison, the characteristics of the standard commercially-available Rh-Fe resistance temperature sensor manufactured by H. Tinsley and Co., Ltd., were also measured. Of the trial-manufactured sensors, the three samples annealed at 800 to 900°C had extremely close resistance-temperature characteristics. When annealing at 700°C, the residual resistance was greater than when annealing at or above 800°C, and it was found that annealing at temperatures exceeding 800°C was required in order to remove the strain generated during the winding of the wire.

3.3 Handy calibration method[6]

In order to calibrate an encapsulated Rh-Fe temperature sensor for temperatures below 30K, a method which

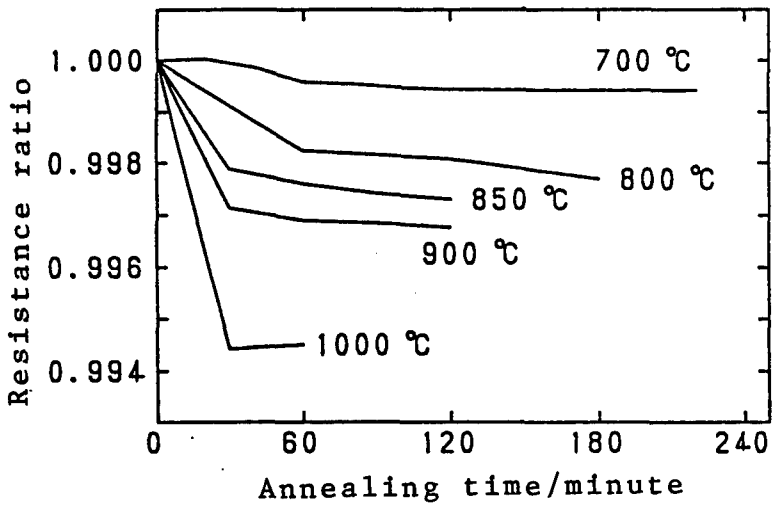

Figure 4. Change in Rh-Fe Wire Resistor for Different Annealing Times[6]

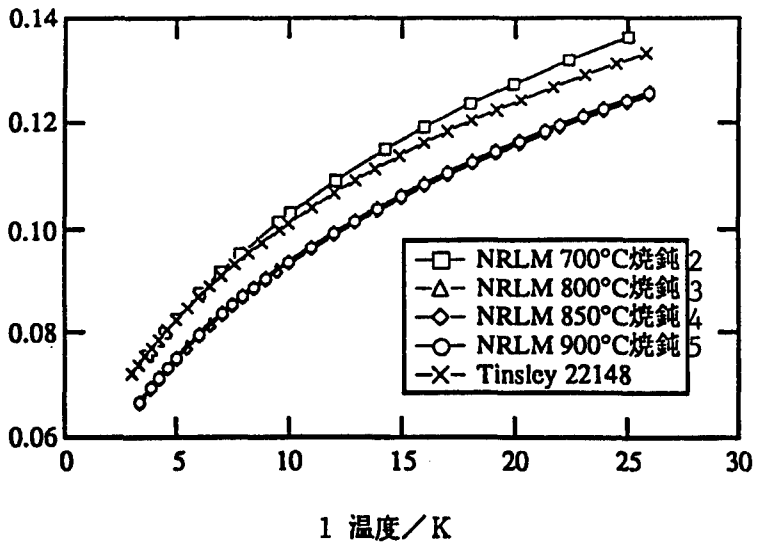

Figure 5. Resistance-Temperature Characteristics of Rh-Fe Wire-Wound Resistance Temperature Sensor
Key: 1. Temperature/K 2. NRLM annealed at 700°C 3. NRLM annealed at 800°C 4. NRLM annealed at 850°C 5. NRLM annealed at 900°C

calibrates at more than 10 sites has been proposed and actually used.[2] However, since only a few fixed temperature points exist in the above temperature range, for a general user who needs the absolute values of the temperature, the calibration method used for this sensor has represented a major barrier.

As described in the previous section, a temperature sensor with very similar resistance-temperature characteristics is obtained when annealing is carried out betweein 800 and 900°C. For sensors with similar characteristics, a calibration method which uses fewer calibration point numbers than the reference functions will be more effective, as will be explained below.

For example, for the measured value W(T) of the resistance-temperature characteristic of a sensor annealed at 800°C, a function W(T) of the following form is applied, and the coefficients A_0, A_1, ..., A_8 are determined by the least squares method.

$$W(T)=\sum_{k=0}^{8} A_k\{\ln(T/K+9)\}^k$$

The function thus determined will be called $W_{ref}(T)$. This function has been designated as the reference function for calibrating the resistance-temperature characteristics of other sensors.

The measured values of W(T) of the respective sensors at three fixed points, e.g., the vapor pressure point of helium in the vicinity of one standard atmospheric pressure, the triple point of hydrogen in equilibrium, and the triple point of neon (approximately 4.2K, 13.8033K and 24.5561K, respectively) are set to equal to

$$W_{fit}(T) = a_0 + a_1 W_{ref}(T) + a_2,$$

to determine the coefficients a_0, a_1 and a_2. The values $W_{fit}(T)$ thus determined are set to be the calibration formulae for the resistance-temperature characteristics of these sensors.

The measurement error $\Delta T = (W(T) - W_{fit}(T))/(dW_{fit}/dT)$ for the case of temperature measurement by each of the sensors, based on the above-mentioned calibration, is shown in Figure 6. The three sensors annealed at and above 800°C are calibrated with errors within 0.5 mK. Although the calibration errors for the two sensors commercially available and the trial-manufactured sensor annealed at 700°C approach 10 mK, the ΔT characteristic is similar for all of them. According to the literature, the annealing temperature for the sensors made by Tinsley is thought to be below 750°C.[5] Accordingly, the dichotomy appearing in Figure 6 can be conjectured as resulting from the differences in annealing temperatures. Since the resistance-temperature characteristics of the sensors annealed at from 800 to 900°C demonstrate only slight differences regarding the influence of the annealing temperature, it may be said that the difference in the characteristic from one sensor to another can practically be corrected by this handy calibration method.

4. Conclusion

In this article, attempts to improve defects involving such things as heat capacity, thermal contact, individual differences and calibration methods in the conventional standard Rh-Fe temperature sensor have been presented. As for the Rh-Fe thin film, it has been confirmed that sensitivity similar to that of a bulk body can be obtained, and hence it can be utilized as a temperature sensor for low temperatures. For wound-type sensors, annealing temperatures of 800°C or higher following wire winding are desirable, as has been confirmed by the use of a molten quartz reel. Since the adoption of annealing temperatures of from 800 to 900°C minimizes the difference among the sensors regarding the characteristics generated by heat treatment, a handy calibration based on one reference function becomes possible. The derivation of a reference function and a handy calibration method which will be applicable to a wider range of sensors, based on the characteristics of many other Rh-Fe sensors, is a task expected to be resolved in the future.

References

1. Preston-Thomas, H., METROLOGIA, Vol 27, 1990 p 3.

2. Rusby, R.L., in "Temperature: Its Measurement and Control in Science and Industry," Vol 5, ed by J.F. Schooley, et al., New York, American Institute of Physics, 1982, p 829.

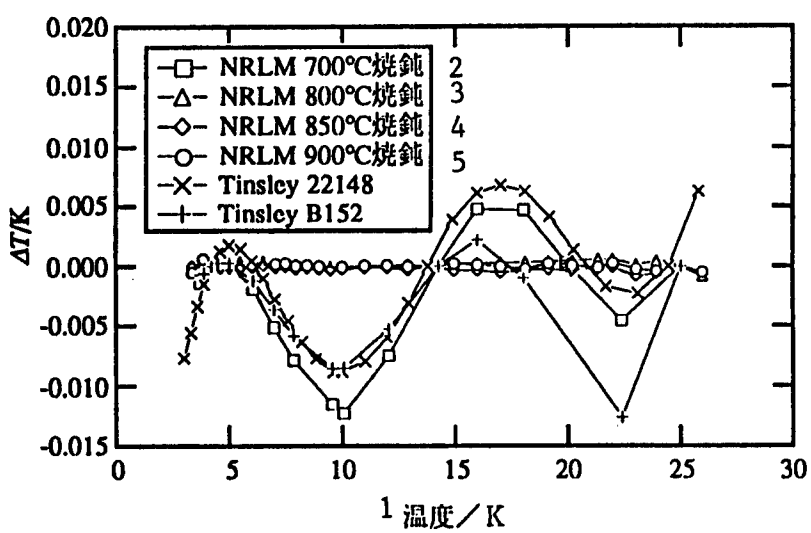

Figure 6. Error for Three-Point Calibration Method Using Reference Function of Rh-Fe Sensor

Key: 1. Temperature/K 2. NRLM annealed at 700°C 3. NRLM annealed at 800°C 4. NRLM annealed at 850°C 5. NRLM annealed at 900°C

3. Shiratori, T., et al., in "Temperature: Its Measurement and Control in Science and Industry," Vol 5, ed. by J.F. Schooley, et al., New York, American Institute of Physics, 1982, p 839.

4. Tamura, O., Sakurai, H., JPN J APPL PHYS, Vol 26, 1987 p L947.

5. Rusby, R.L., in "Temperature: Its Measurement and Control in Science and Industry," Vol 4, ed. by H.H. Plumb, et al., Pittsburgh, Instrument Society of America, 1972, p 865; Rusby, R.L., in "Temperature Measurement 1975," ed. by B.F. Billing and T.J. Quinn, London, Institute of Physics, 1975, p 125.

6. Tamura, O., Sakurai, H., to be published in CRYOGENICS, Vol 31, 1991.

Superconducting Magnetic Sensor SQUID

926C0010D Tokyo SENTAN GIJUTSU OYO SYMPOSIUM in Japanese 3 Sep 91 pp 21-28

[Article by Hisashi Kato, Electrotechnical Laboratory, currently on TDY to Superconducting Sensor Laboratory]

[Text]

Introduction

When a nerve or muscle is activated, ions flow within and without the cells, generating a weak current. As learned in electromagnetism, a current generates a magnetic field in its surroundings, extending even outside the organism. In general, the position and strength of the source generating the magnetic field can be determined by observing the magnetic field. If one can determine the position and direction of the source of the magnetic field in an organism by externally observing the magnetic field generated by the organism, it will be possible to learn about the activities within the organism without intruding. In reality, however, unless a highly sensitive magnetic field sensor is provided, the above-mentioned detection cannot be carried out because the magnetic field generated by the organism is extremely weak.

A highly sensitive magnetic sensor called SQUID has been developed by employing the Josephson effect and the Meissner effect, which are the fundamental laws of superconducting electronics, making possible the detection of extremely weak magnetic fields.[1)]

The Meissner Effect

Let us consider a ring of a superconductor. If one attempts to let a magnetic flux infiltrate the ring, it cannot be accomplished. This is because a current (shielding current) is generated within the ring, excluding the external magnetic flux. This phenomenon is called the Meissner effect (Figure 2).[2),3)]

Josephson Junction and Josephson Effect[2),3)]

A superconductor with one very thin portion or a body obtained by inserting a thin insulating layer between two

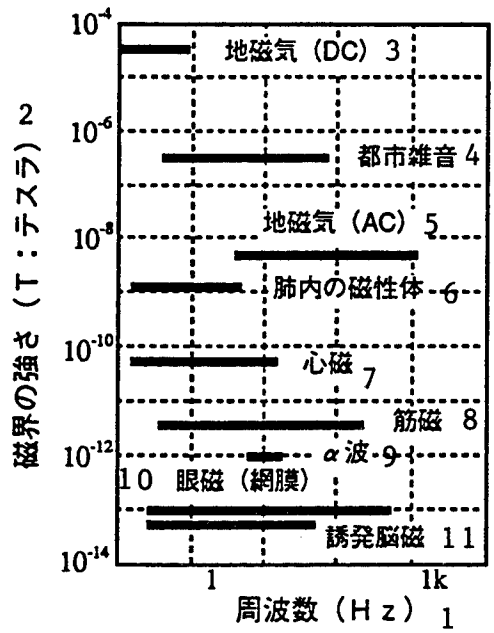

Figure 1. Strength and Frequencies of Various Magnetic Fields

Key: 1 - Frequency (Hz); 2 - Magnetic field strength (T: tesla); 3 - Geomagnetism (dc); 4 - City noise; 5 - Geomagnetism (ac); 6 - Magnetic body in lung; 7 - Cardiac magnetism; 8 - Muscular magnetism; 9 - α wave; 10 - Ophthalmic magnetism (retina); 11 - Induced cerebral magnetism

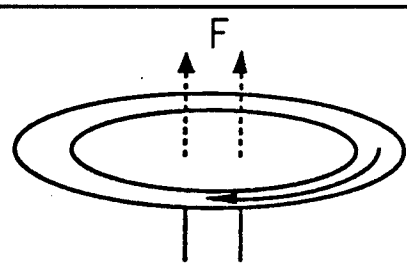

Figure 2. Meissner Effect

A shielding current flows in the ring in a direction which excludes the magnetic flux penetrating the ring.

superconductors is called a Josephson junction (Figure 3). Even when there is no potential difference on either side of a Josephson junction, a superconducting current (Josephson current) can flow. This effect is called the Josephson effect. However, this current has an upper current (critical current: Ic), beyond which the superconducting state is destroyed and the voltage switched.

Principle of SQUID[2),3)]

The principle of SQUID can be explained in terms of the Josephson and Meissner effects. Of the two SQUID

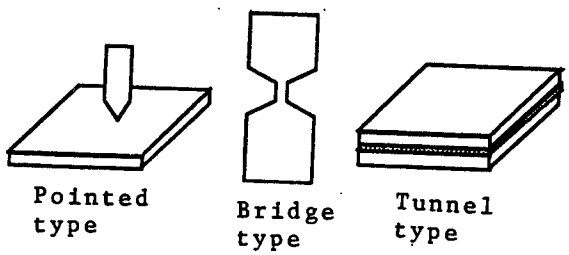

Figure 3. Examples of Josephson Junctions

types, i.e., the DC-SQUID and RF-SQUID, a description will be given here of the DC-SQUID, which currently represents the mainstream of development. (In the following, SQUID will be used for DC-SQUID.)

In a SQUID element, two Josephson junctions are provided in a doughnut-shaped ring made of a superconductor (Figure 4), and a Josephson current flows between the Josephson junctions. On the other hand, when an external magnetic flux attempts to enter the ring, a shielding current flows in the ring in a direction excluding the magnetic flux. However, in the case of a SQUID ring, since a shielding current flows, a magnetic flux which is an integral multiple of a constant value Φ_0 can enter the ring. Here, Φ_0 is a physical constant, termed a magnetic flux quantum, and since its value is as small as approximately 2.07×10^{-15} Wb, it is possible to use a SQUID to detect a weak magnetic flux.

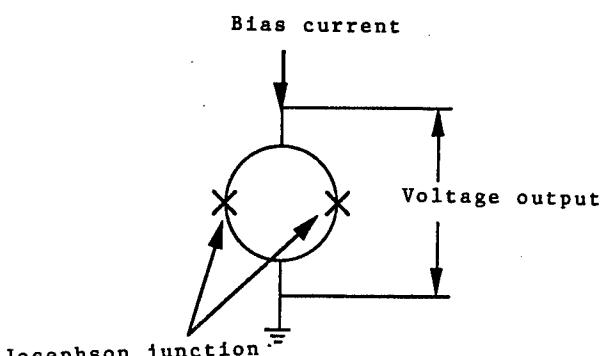

Figure 4. Equivalent Circuit for SQUID

The shielding current flows in a direction that encircles the ring, and hence its directions at the two Josephson junctions are opposite each other. Accordingly, the current that flows in one Josephson junction is greater by an amount corresponding to the shielding current, and the apparent critical current is correspondingly smaller by that amount. The critical current I becomes a periodic function of the external magnetic flux Φ penetrating the ring, and can be represented by

$$I = 2I_0 \text{ absolute value of } \cos(pF/F_0 \qquad (1)$$

In the above, I_0 is the maximum current (critical current) per Josephson junction for $\Phi = n\Phi_0$ (n = 1, 2, ...), and is usually several dozen microamperes.

In order to operate the system as a SQUID, a bias current which is somewhat greater than the critical current is passed through the SQUID. A voltage is generated across the ends of the SQUID, but when a magnetic flux enters the ring, the critical current is changed according to Equation (1), making the current-voltage characteristic vary in the same manner, and thus the change in the magnetic flux can be detected as a change in voltage (Figure 5). In this case, the current becomes minimal for every $1/2\Phi_0$, while the output voltage is maximized. Since the output voltage changes periodically, a linearization device is required for the actual detection of the magnetic flux.

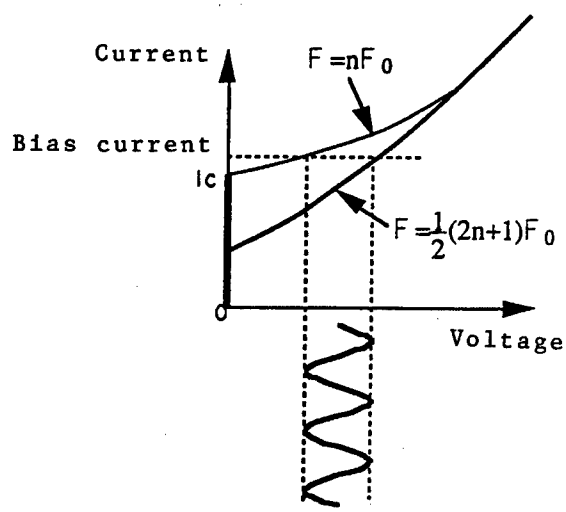

Figure 5. Current-Voltage Characteristics and Output of SQUID

Tunnel Junction

As shown in Figure 3, Josephson junctions include the pointed type, in which a portion of the superconductor is extremely thin, i.e., needle form, the bridge type which has a "constricted part" in a portion of the superconductor, and the tunnel type which has a thin insulating layer between superconductors. However, it is still difficult to manufacture robust elements with the bridge and pointed types, and they are not appropriate for integration due to their structures.

On the other hand, with the tunnel type junction, it has become easy to manufacture a large number of robust elements with uniform characteristics at one time by using improved thin film formation technology and the

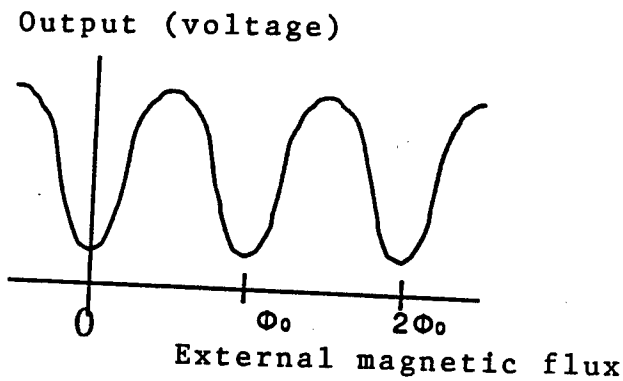

Figure 6. Output Characteristics of Conventional SQUID

fine geometry technology achieved in recent years through the advancement of semiconductor technology. Making full use of thin film formation technology, the tunnel type Josephson junction (tunnel junction) is currently becoming the mainstream. The current in the tunnel junction reveals itself as a quantum mechanical effect in which the superconducting electrons (Cooper pairs) cause the tunneling effect. Its current-voltage characteristic (characteristic of voltage that appears across both ends of the junction when a current is passed through the junction) is very different from those of the bridge and pointed types and exhibits hysteresis as shown in Figure 7. In the tunnel junction, when the current flowing in the junction exceeds the critical current I_0, a finite current, called a gap voltage, occurs (depends on the superconductor, usually several millivolts). In this way, a tunnel junction is a kind of switching element and can generate substantial voltage.

However, since the presence of hysteresis is undesirable for SQUID operation, it is necessary to improve the current-voltage characteristics to ones similar to those for the bridge and pointed types (shown in Figure 5). For this reason, when the SQUID is used as a tunnel junction, the hysteresis is eliminated by inserting a resistor (shunt resistor) in parallel with the junction. As a result,

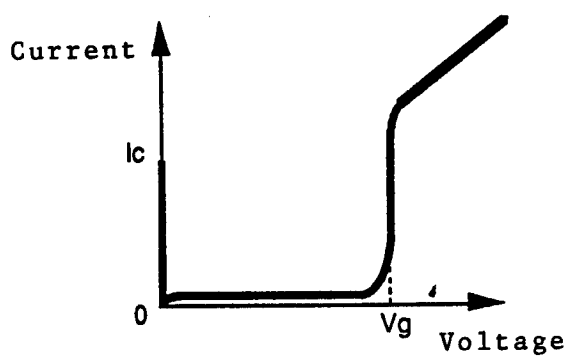

Figure 7. Current-Voltage Characteristics of Tunnel Junction

the output voltage becomes lower and the large gap voltage cannot be fully employed. While most SQUID's currently being developed have adopted this method, the output value is low, i.e., several dozen microvolts.

Actual SQUID Fluxometer

With a SQUID main body alone with a diameter on the order of several micrometers, the magnetic flux that can be picked up is relatively limited. In reality, a coil (pick-up coil) for detecting magnetic fields is attached externally and a SQUID fluxometer is constructed so that a magnetic field is transferred to the SQUID through an input coil connected to the pick-up coil. Moreover, since the output voltage of the SQUID and the magnetic flux are related, changing periodically, it is necessary to correct the relationship, making it proportional, by using an electrical circuit. For this purpose, a feedback coil is placed in the vicinity of the SQUID and a current is passed through the coil, generating a magnetic field that restores the output voltage to zero. By reading the feedback current from the outside by converting the current to a voltage, it becomes possible to obtain output that is proportional to the magnetic flux (Figure 8).

This is referred to as the flux locked loop operation (FLL) method, and a magnetic flux density resolution on the order of 10^{-14} T can be obtained by adopting this configuration. Moreover, by extending the frequency characteristic of the SQUID itself to the high frequency region, it is possible to enhance the time resolution of the fluxometer by improving the FLL's slow electronic circuit rate.

Conventional SQUID System

A SQUID system with about 30 channels has already been developed. These SQUID's output the change in the magnetic field as a change in voltage, as mentioned above, with four to six signal lines required for one SQUID. However, since a SQUID is operated at the extremely low temperature of 4.2K, from the viewpoint of avoiding heat infiltration, it is necessary to minimize, as much as possible, the number of signal lines required to take the signal to room temperature. Accordingly, for the currently available SQUID's, there is a limit to the number of realizable channels (number of signal lines exceeds 1,200 for 200 channels). To reduce the number of signal lines, although methods, such as digitizing the electrical signal from the SQUID at helium temperature, then multiplexing it, are being considered, no method has yet been established. (The development of a different type of SQUID which will output the signals as digital signals from the beginning has recently been initiated.)

Another major problem involves noise and resolution. In order to be able to detect extremely weak magnetic fields, the noise level of the entire circuit, including the SQUID, has to be lowered sufficiently. In the case of the magnetic field around the brain, which is the weakest of the biological magnetisms, since it is on the order of

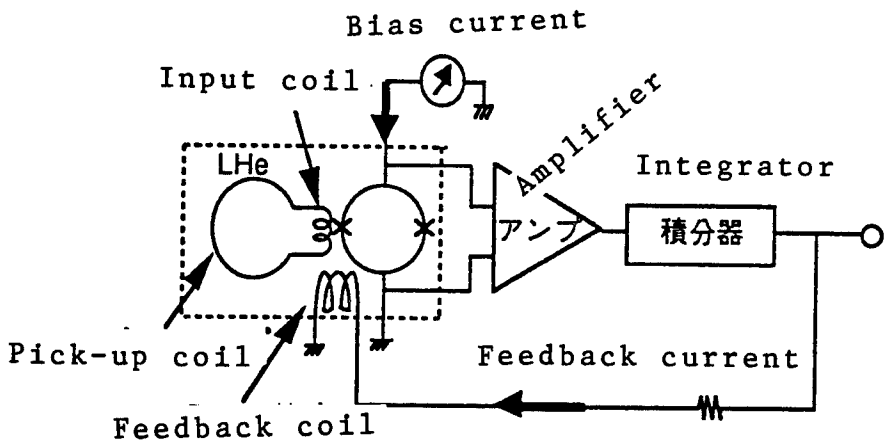

Figure 8. Example of Configuration of SQUID Fluxometer

ten-odd femtoteslas, a sensitivity of this order requires a SQUID fluxometer to have still higher sensitivity. In order to enhance the sensitivity by lowering the noise, it is advantageous to increase the SQUID output level. Considering SQUID fluxometers with even higher sensitivity, the output level (several dozen microvolts) of the currently available SQUID is approaching its limits.

Relaxation Oscillating SQUID

By connecting a resistor and a coil in parallel instead of a shunt resistor to a SQUID having hysteresis (Figure 9) (relaxation oscillating SQUID (ROS)), and passing a bias current within the range of certain conditions, the SQUID starts to oscillate. Since the oscillation frequency at this time changes periodically in response to the magnetic flux penetrating the SQUID ring, a SQUID is obtained which can output the change in magnetic flux as a change of frequency (Figure 10). Since the output is frequency, it is anticipated that multiplexing can be achieved relatively easily through digitization and the existing FM technology, and the system is considered appropriate for use in multi-channel SQUID systems. Moreover, since the noise due to frequency is essentially low when compared with the noise resulting from current or voltage, there is a possibility that a highly sensitive SQUID will be realized.

The ROS first developed by M. Mück and H. Heiden, et al., adopted the bridge-type Josephson junction (strictly speaking, it is not a Josephson junction).[4] The bridge type does not have intrinsic hysteresis, but instead utilizes the hysteresis resulting from the heat cycle. Therefore, it was necessary to control the temperature precisely in order to obtain a stabilized hysteresis. However, a problem occurred in that the thermal hysteresis exhibited a slow response speed (several dozen MHz at the most). On the other hand, the tunnel junction is appropriate for ROS because it has an intrinsic hysteresis. Moreover, since it is not necessary to eliminate the hysteresis, it is possible to take out the gap voltage output on the order of several millivolts. Furthermore, it makes it possible to reduce the noise since the response speed is high (several hundred GHz).

ROS Principle

A certain constant bias current greater than the critical current is passed through the ROS. The SQUID is

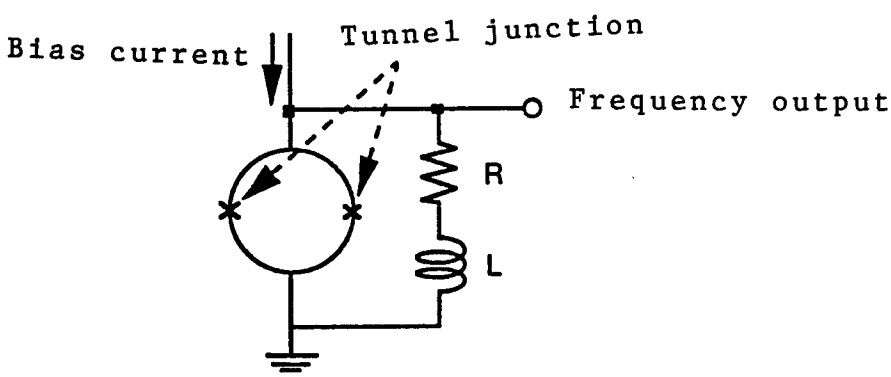

Figure 9. ROS Equivalent Circuit

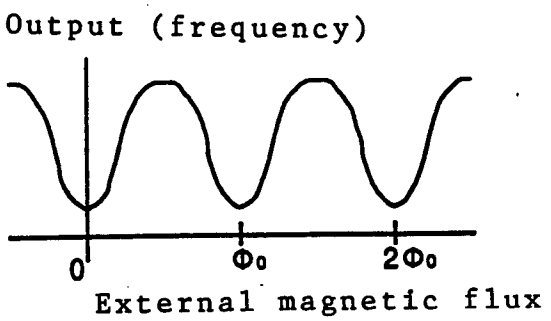

Figure 10. ROS Output Characteristics

shifted to the finite voltage state when the current exceeds the critical current, returning to the superconductive state if the current is consumed on the shunt side. By repeatedly alternating this switching, the system enters the oscillating state. The oscillation waveform is not sinusoidal, but exhibits so-called intermittent oscillation (Figure 11). Although the oscillation frequency can be varied by changing the bias current, oscillation can only be initiated when the bias current is within a certain range where the conditions for oscillation are determined by the intrinsic properties of the tunnel junction and the magnitude of the resistor. The magnitude of the oscillation frequency is on the order of the reciprocal R/L of the time constant that is approximated by the resistance and inductance of the coil.

As an external magnetic flux penetrates the ROS, the critical current changes, as mentioned earlier, and, as a result, the hysteresis loop of the current-voltage characteristic changes, manifesting itself as a change in frequency. Intuitively, the change is due to the change in the distance along the loop, and the frequency reaches a maximum value when the hysteresis loop becomes minimal for every $1/2\Phi_0$ (Figure 12).

Actual ROS[5)]

In our laboratory we used thin film technology to experimentally manufacture a ROS employing tunnel junctions and, by varying the bias current, were successful in

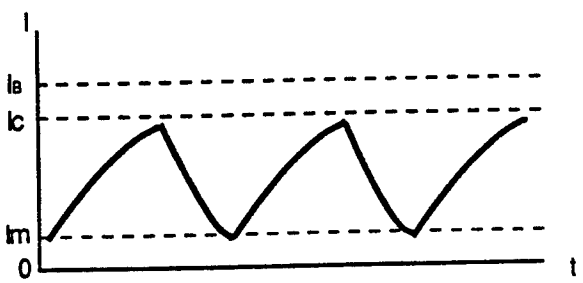

Figure 11. ROS Oscillation Waveform (for Current)
I_B is the bias current, while I_m is the minimum critical current.

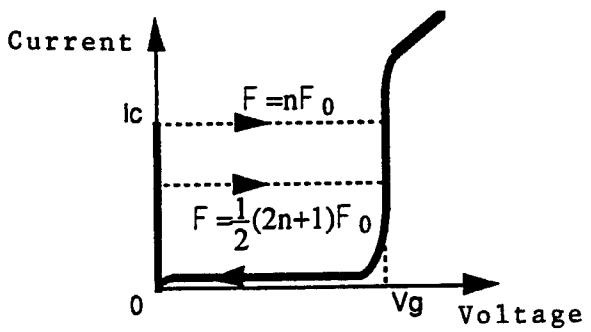

Figure 12. ROS Current-Voltage Characteristics

oscillating the system over a wide frequency range of from 40 MHz to 1 GHz. The corresponding range of the bias current was 0.2 to 0.6 mA. The waveform of the oscillation spectrum is very sharp and the frequency stability is also extremely good (Figure 13).

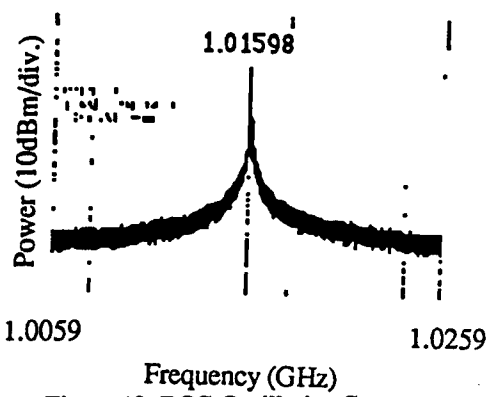

Figure 13. ROS Oscillation Spectrum

Moreover, the oscillation frequency changes periodically with the external magnetic flux (Figure 14), with a maximum change of up to 1.6 GHz for a flux of $1/2\Phi_0$ at

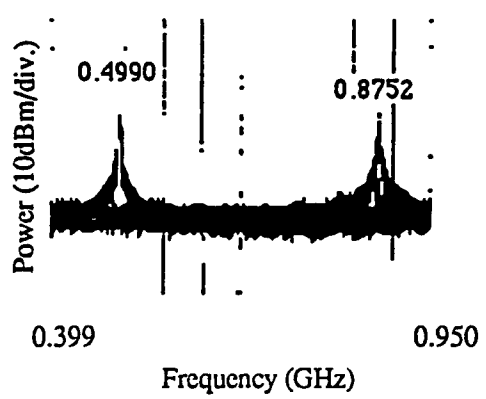

Figure 14. Change in Oscillation Frequency with Magnetic Flux

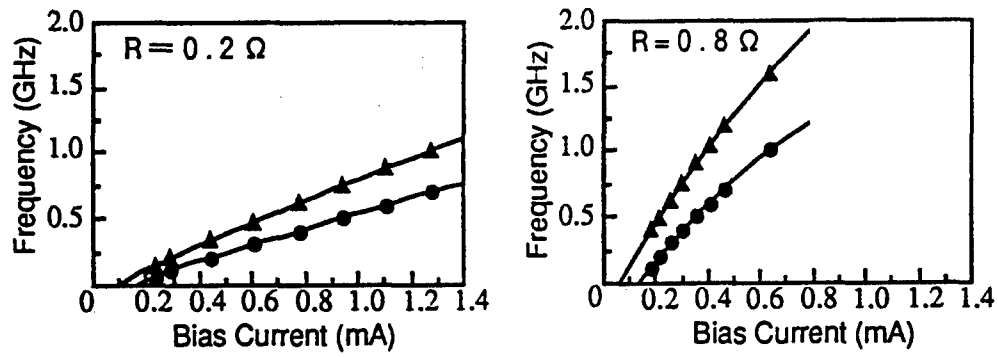

Figure 15. Bias Current Dependence and Change for Magnetic Flux of Oscillation Frequency
solid circle: F = 0, solid triangle: F = 1/2F0

the fundamental frequency of 1 GHz. Figure 15 shows the change in frequency for magnetic fluxes of $\Phi = 0$ and $1/2\Phi_0$ when the bias current is changed.

The noise level (SSB phase noise) estimated from these results is very low, obtaining an ROS resolution of about $10^{-7}\Phi_0/Hz^{1/2}$.[6] This represents a value which is one order of magnitude better than that obtained for the conventional SQUID.

From the results of this experiment it is definitely thought that a new ROS fluxometer can be expected whose performance will exceed that of the conventional SQUID.

Problems and Future of ROS

The ROS demonstrates excellent characteristics, but, as listed below, many problems remain to be resolved, including those involving peripheral technologies, if it is to be extended to a multichannel SQUID system.

(1) In order to further enhance the resolution, the higher the oscillation frequency the better. For processing high frequency signals, however, an advanced high frequency technology is required. For example, problems related to transmission lines, technology for reducing the high frequency to low frequency by mixing down, etc., must be studied.

(2) Since the ROS output power is a very low value of several hundred nanowatts, it is necessary to amplify it in one way or another. Moreover, considering noise and integration, amplification (amplification that employs the HEMT or Josephson technology) at low temperatures is desirable.

(3) The digitization and multiplexing of the frequency output are still being sought at this moment. For example, a method of multiplexing by changing the frequency little by little for various channels is being studied. For that purpose, it is necessary to introduce the so-called existing FM technology. Moreover, in order for signals to be extracted from low temperatures by employing as few signal lines as possible, it is necessary that low temperature signal processing be conducted. The development of analog and logic circuits employing Josephson technology will also become important. It seems that only by solving these problems will it become possible for SQUID systems with several hundred channels to be realized.

Summary

Currently, the development of multichannel systems by employing the conventional SQUID is progressing, and the world seems to have entered the channel number race. However, in comparison with the conventional SQUID whose output is voltage, when viewed from various standpoints, ROS, whose output is a frequency, seems to be more adaptable to more advanced multichannel systems. However, for its realization, not only the development of key devices for detecting the magnetic field, but also the development of peripheral circuits is inevitable. It is necessary to establish many technologies, such as Josephson electronics technology, communications, and computer technology.

References

1. Kato, H., "Auditory Cerebral Magnetic Field," J ACOUST SOC JAPAN, Vol 44, 1988 p 3.

2. Kitamura, T., "Experiment of Science," Supplement, Vol 30 Nos 10-12.

3. Clarke, J., PARITY, Vol 1 No 9, 1986.

4. Mück, M., et al., APPL PHYS A, Vol 46, 1988 p 97.

5. Kawai, J., Uehara, G., et al., SQUID '91 (1991) (to be published).

6. Kondo, Y., Uehara, G., et al., EIC Conference SCE91-4, 1991.

Molecular Composite Systems With Sensing Capabilities

926C0010E Tokyo SENTAN GIJUTSU OYO SYMPOSIUM in Japanese 3 Sep 91 pp 31-35

[Article by Fumio Mizutani, Textile Polymer Materials Laboratory]

[Text]

1. Introduction

In living things, highly advanced molecular recognition and response functions accompanied by amplification, control, etc., are manifested by ingenious combinations of molecular functions of enzymes, etc. For example, in the process in which a trace hormone demonstrates a conspicuous physiological activity, a chain of molecular functions occurs, including the coupling of the specific protein (receptor protein) and the hormone → the activation of the enzyme molecules that exist in the neighborhood → the production of a large quantity of output (second messenger) by enzyme reactions. The construction of sensor systems which imitate or go beyond such functions are expected to represent important research problems toward the 21st Century.

By recognizing such sensing systems as the object, we have already begun the development of systems which not only are able to fully exhibit the individual functions of enzyme molecules, etc., but also make possible a delicate functional linkage between molecules or between molecules and an instrumental device, and we have been engaged in the special research referred to in the title of this article since FY90. In the following, as a part of our approach to the project, we will discuss the structure of enzymatic membranes with chemical amplification functions, the technology required for realizing electron transfer between enzymes and electrodes as well as that required for the electrical control of enzymatic activity, and the construction of an optical sensor that uses the purple membrane. Needless to say, the construction of "molecular composite systems with sensing capabilities" will require the accumulation of wide-ranging and highly-advanced technologies. In that sense, some of our attempts are still in their infancy and the distance behind the ideal situation is still very great. Nonetheless, we expect novel systems, such as chemical and optical sensing systems with high sensitivity and dynamic range, etc., to be developed as a result of these attempts.

2. Structure of Chemical Amplification Enzymatic Sensors

The chemical amplification process, during which numerous molecules are produced due to a chain of chemical reactions involving a small number of molecules, is an indispensable process which employs chemical substances as the carriers of information, as mentioned above. On the other hand, this concept can also be applied to enhance the sensitivity of chemical analysis. The principle of operation of the chemical amplification enzymatic sensor (lactic acid sensor) previously developed by us is shown in Figure 1. While, in the ordinary lactic acid sensor, lactic oxidase (LOD) is used separately as the enzyme, in this sensor LOD and lactic dehydrogenase (LDH) are used simultaneously. The lactic acid consumed through the action of LOD is regenerated by the action of LDH. During the process of repeating the consumption/regeneration cycle, one molecule of lactic acid consumes a large number of oxygen molecules. Accordingly, a substantial sensor response (current change in the oxygen electrode) is obtained in comparison with that of the ordinary lactic acid sensor (one molecule of lactic acid consumes one molecule of oxygen). The amplification factor of the sensor response is larger for the greater enzymatic activity in the immobilized membrane. The maximum value for the amplification factor obtained empirically by us is around 300 (optical crosslinking polymer[2]) is utilized as the immobilizing material. The enzymatic activity within the immobilized membrane is on the order of 100 U/cm^3), and the detection sensitivity becomes higher corresponding to the amplified response level, reaching several nanomols. We are aiming at the realization of sensors with sensitivity less than 1 pM by searching for materials that carry the enzyme at high activity, and at the preparation and utilization of fused protein in which two enzymes are compounded when their activation centers are approaching each other's. In order to realize the desired characteristics *in vitro*, the preparation of such fused proteins is considered to be a major task for the future.

3. Communications Between Enzymes and Electrodes

The oxidation of the matrix by an oxidase such as LOD includes the matrix oxidation by a cofactor in the enzyme and the oxidation and regeneration of the reduction-type cofactor by oxygen, as follows:

$$RH_2 + E/FAD \rightarrow R + E/FADH_2 \quad (1)$$

$$E/FADH_2 + O_2 \rightarrow E/FAD + H_2O_2 \quad (2)$$

In the above, RH_2 and R represent the matrix and its oxidized version, while E/FAD and $E/FADH_2$ represent, respectively, the states in which the oxidation and reduction types of the cofactor flavin adenine dinucleotide are bonded to the enzyme molecule E. Here, if the regeneration of the oxidation-type cofactor is carried out by electrolytic oxidation,

$$E/FADH_2 \rightarrow E/FAD + 2H^+ + 2e^-, \quad (3)$$

instead of by the above two equations, then a sensor can be constructed which can simultaneously detect the enzyme reaction speed by means of the electrolysis current. However, the cofactor is "enclosed" by the enzymatic molecule chain, and electron transfer with the electrode does not ordinarily take place. For this reason, a substance (mediator, M^+/M) which mediates the electron transfer between the enzyme and the electrode is utilized.[3]

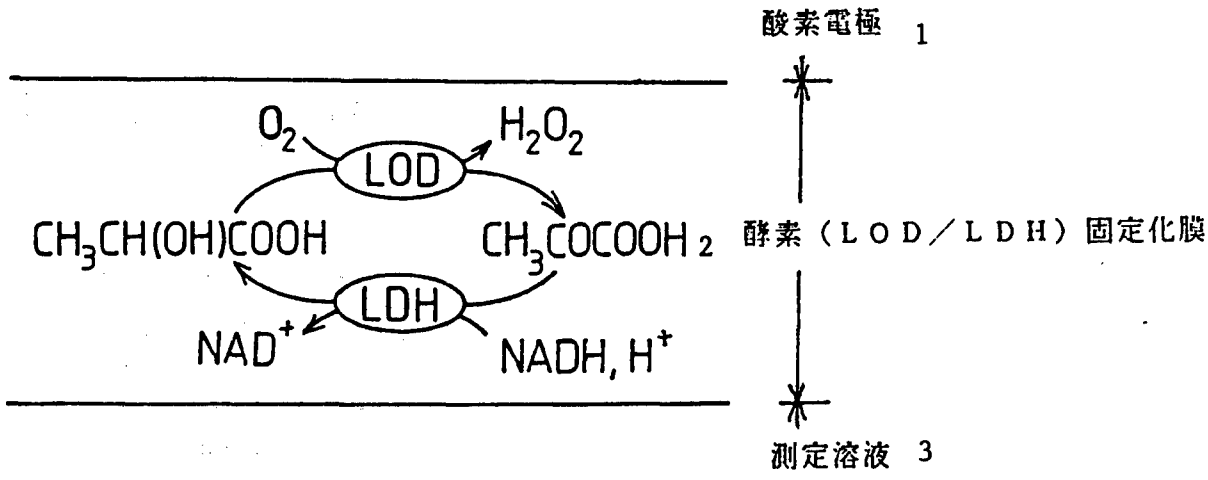

Figure 1. Chemical Amplification Lactic Acid Sensor Using Enzyme Cycling

$CH_3CH(OH)COOH$: lactic acid; $CH_3COCOOH$: pyruvic acid; NADH: reduction nicotinamide adenine dinucleotide; NAD^+: oxidation nicotinamide adenine dinucleotide. Key: 1. Oxygen electrode 2. Enzyme (LOD/LDH) immobilized membrane 3. Measurement solution

$$E/FADH_2 + 2M^+ \rightarrow E/FAD + 2M + 2H^+, \quad (4)$$

$$2M \rightarrow 2M^+ + 2e^- \quad (5)$$

In constructing a sensor which utilizes such a mediator, it is desirable to immobilize the enzyme and the mediator. On the other hand, since the electron transfer between the immobilized sites is generally fairly slow, it is necessary to devise some sort of method to promote it. We found that the utilization of a conductive carrier is appropriate for this purpose, and used a conductive polymer, platinum black, carbon paste, etc., as the immobilizing carrier.[4] We also found that, in some cases, electron transfer could take place without the presence of a mediator when a method was employed in which a conductive polymer chain served as a molecular wire between the enzyme molecule and the matrix electrode.[5]

An electrochemically-active water soluble polymer material is thought to be useful as a mediator since it is easy to trap it in the electrode/semipermeable membrane by covering the electrode surface with the semipermeable membrane, and it is possible to shuttle electrons by means of the diffusion between the enzymatic molecules and the electrode. It was found that polypeptides which had ferrocene as a side chain acted as mediators for glucose oxidase.[6]

4. Electrical Control of Enzymatic Activity

As an example of the relationship between the enzyme and the electrode, one can point out the electrical control of the enzymatic activity. In an electrode system which utilizes a mediator, the reaction rate of Equation (5) changes with a change in the electrode potential. This, however, can also be viewed as the activity of the enzyme having been changed. That is, it corresponds to having controlled the enzymatic activity by changing the potential. Moreover, in a conductive polymer matrix, the charged state is changed by the potential. For example, when the membrane enters the doped state and finds itself with a positive charge, the concentration within the membrane of the negative-charged matrix is increased (or the transfer speed into the membrane is increased), and the enzymatic activity is increased over that of the undoped state with no charge.[7]

Not only such control of the "apparent" enzymatic activity, but also the search for an enzymatic activity control system of the form which causes a conformational change, etc., of the enzyme molecules is also in progress.

5. Structure of Enzyme Sensor Having Wide Dynamic Range

Using the chemical amplification enzyme sensor discussed in Section 2 will enable an enzymatic sensor having a wide dynamic range to be fabricated by considering the fact that the amplification factor depends significantly on the enzymatic activity in the immobilized membrane, and in accordance with the discussion of the possibility of electrical control of the enzymatic activity presented in Section 4. For example, a structure was obtained which makes it possible to measure the matrix electrode current by using an electrode buried in the enzyme membrane, as shown in Figure 2, while controlling the amplification factor (and the measurable concentration range). Its structure is quite similar to that of a triode tube and its operation is also similar to that of the triode. The fabrication of an enzymatic sensor having a wide dynamic range comparable to that of a pH electrode is anticipated.

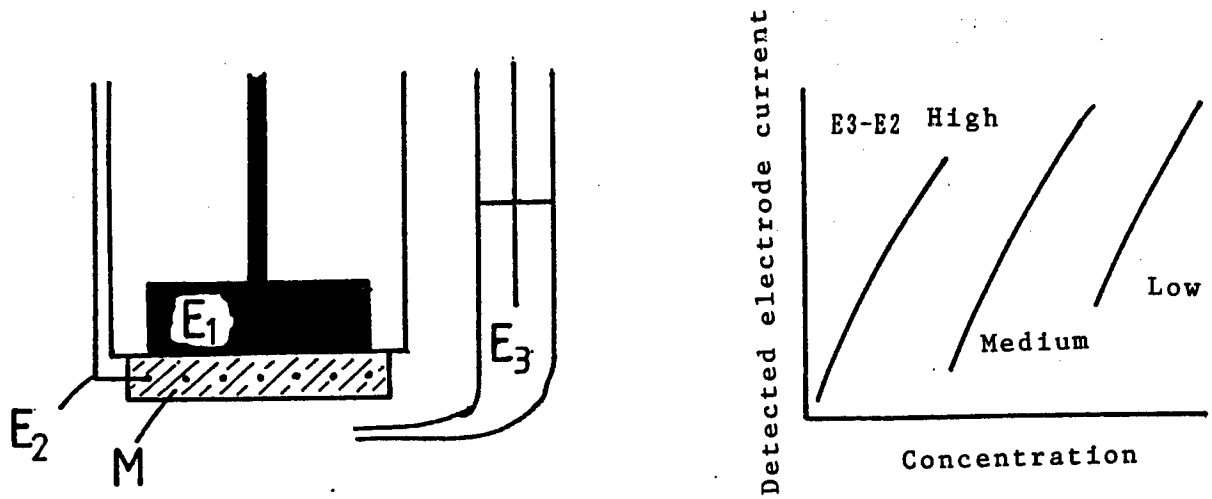

Figure 2. Example of Enzyme Sensor Having Wide Dynamic Range and Response Characteristics.

E_1: detection electrode; E_2: electrode for controlling enzyme activity; E_3: reference electrode; M: enzyme membrane. If the potential between E_2 and E_3 is changed, the enzymatic activity in the enzyme membrane is changed, and, accordingly, the amplification factor and range of measurable component concentration are changed. In other words, it is possible to obtain sensors that cover a wide concentration range by controlling the potential.

6. Optical Sensor Modeled After Vision

A purple membrane is a biological membrane produced by Halobacterium halobium which consists of bacteriorhodopsin and lipid. Since bacteriorhodopsin molecules with optical proton pumping functions are arranged and oriented to form two-dimensional crystals within the purple membrane, it is possible to regard the purple membrane itself as an optical signal conversion element with previously-arranged functional molecules. By utilizing an electrodeposited membrane of a purple membrane, it is possible to obtain an optical sensor which exhibits a photocurrent action spectrum that resembles the specific visual sensitivity curve of the human eye.

As optical sensors that simulate the amplification function of the human visual system, it is possible to consider high sensitivity system configurations that utilize the following mechanisms: the production of an electrode active substance by the chain of light absorption by bacteriorhodopsin → a change in proton concentration → the activation of an enzyme (phosphatase, etc.) → enzyme reactions or the actuation of a biochemical light emitting system → the measurement of an amplified electrochemical signal or optical signal, and we have already begun to examine element technologies for the system configuration.

7. Conclusion

In the above, we have presented our approach to creating sensing systems which will imitate the functions of living things by employing molecules as the carriers of information and energy, while making it possible to communicate with electronic systems that use electrons as the carriers of information and energy. Despite the fact that, as was mentioned earlier, the gap between the goal and reality is large, we intend to continue the research to lessen this gap, although it may represent only a small step forward.

References

1. Mizutani, F., et al., ANAL CHIM ACTA, Vol 177, 1985 p 153; Mizutani, F., et al., J CHEM SOC JPN, 1987 p 531.

2. Ichimura, K., J POLYM SCI, POLYM CHEM ED, Vol 22, 1984 p 2817.

3. Mizutani, F., Asai, M., in D.L. Wise, ed., "Bioinstrumentation," Boston, Butterworths, 1990, p 317; Mizutani, F., Yabuki, S., in S. Yamauchi, ed., "Chemical Sensor Technology," Vol 4, in press.

4. Mizutani, F., Asai, M., BULL CHEM SOC JPN, Vol 61, 1988 p 4458; Mizutani, F., et al., BULL CHEM SOC JPN, in press.

5. Yabuki, S., Shinihara, H., Aizawa, M., J CHEM SOC, CHEM COMMUN, 1989 p 945; Yabuki, S., Mizutani, F., Katsura, T., to be published.

6. Mizutani, F., Asai, M., DENKI KAGAKU, Vol 56, 1988 p 1100; Kunugi, S., et al., POLYM BULL, Vol 23, 1990 p 57; Iijima, S., et al., to be published.

7. Yabuki, S., et al., J ELECTROANAL CHEM, Vol 227, 1990 p 179; Yabuki, S., Mizutani, F., Asai, M., BIOSENS BIOELECTR, Vol 6, 1991 p 311.

Biomimetic Chemical Sensors

926C0010F Tokyo SENTAN GIJUTSU OYO SYMPOSIUM in Japanese 3 Sep 91 pp 37-45

[Article by Yutaka Ishigami, Chemical Technology Research Laboratory]

[Text]

1. Introduction

Since Bangham's clarification that phospholipid forms a cellular liposome as the matrix lipid of a biological film, research on liposomes has been focused on the pursuit of the possibility of DDS. Namely, the sustained releasing and efficacy persistence of drugs which are made into ultra microcapsules by enclosing drugs in liposomes, and the efficacy augmentation and prevention of side effects by targeting those utilizing antigen-antibody reactions, etc., have been attempted. However, in practical applications, the use of cosmetics (including liposome prescriptions) employing phospholipid is proceeding as one aspect of cosmetic-oriented research.[1)-3)] The author and his colleagues have been pursuing the possibility of applying liposomes to chemical sensors and DDS through a biomimetic approach. In this paper, research on the construction of intelligent systems that imitate living things which is being carried out by the author's group will be introduced.

2. Formation of HLB and pH-Dependent Vesicles by Biosurfactants

Liposomes, representing an intrinsically unstable system, alter the composition of phospholipid homologs, and since the phase transition temperature is changed by the added substance, it is possible to have temperature-dependent controlled release. For the vital film system used as a model, it has been determined that phospholipid and cholesterol exist in equal molar numbers in the film of erythrocytes, that the phospholipids of bacterial cellular membranes have no phosphatadyl choline and consist mainly of phosphatadyl ethanolamine,[4)] and that the phospholipid homologs in the inner and outer layers of the phospholipid bimolecular membranes in small cellular organs are distributed asymmetrically, where, although more phosphatadyl inositol, sphingomyelin and cardiopyrene are found in the inner layer, [5)] generally, phosphatadyl choline and phosphatadyl ethanolamine are distributed in the outer layer, etc., and it is believed that adjusting the fluidity, the degree of dissociation of dissociative groups and the barrier capability of the membrane, etc., is possible.

As for living membranes with phospholipid bimolecular membrane structures, it has been determined that thermal bacteria and some marine bacteria have glyceryltetraether and glycolipids, respectively, as the matrix phospholipids. In addition, there are many examples of amphipathic compounds originating from living organisms independently forming vesicles (ufasomes), such as the formation of vesicles by oleic acid at pH 8.[6)] The author and his colleagues have also confirmed the vesicle formation of amphipathic cellular membrane components of procaryote, rhamnolipids A and B, spicryspolates amd cane sugar diester.[7)-9)] By the geometrical shape of the phospholipid molecules, the vesicle formation capabilities of phosphatadyl choline, sphingomyelin, phosphatadyl ethanolamine, etc., that have large polar groups, are emphasized.[10)] The author and his group demonstrated this by citing the case of HLB, an amphipathic molecule, which becomes the determining factor of vesicle formation. Namely, in Figure 1, the rhamnolipid has a nonionic sugar part and an anionic carboxylic group as the hydrophilic groups, and since its water solubility depends on the hydrophilicity of the sugar part, using transmission electron microscopy employing negative coloring, we confirmed that the rhamnolipid forms a vesicle in a semitransparent aqueous solution (pH 4.3 to 5.8). Moreover, the presence of lamella liquid crystal at pH near 6.2 and amorphous lipid particles at pH 6.4 were observed by a fluorescence microscope using an amphipathic fluorescent dyestuff. Further, the presence of micelles at pH 7.2 was observed by the static light scattering method, and the association molecular number obtained for the rhamnolipid was B:8:A:56. Such a pH dependency transformation of the molecular aggregate form resembled, in principle, the cell division and membrane fusion of rhamnolipid B, as did liposome preparation employing the micelle or fusion method that uses acidic phospholipids. Moreover, we have demonstrated that among alkali metals and alkylamines, HLB of both 2-ethylhexyl amine and n-hexyl amine salts can be adapted for vesicle formation as the ion to be paired with the carboxylic groups in spicrysporic acid [(4S,5S)-4,5-dicarboxy-4-pentadecanolide] and in the open ring body of its lactone ring. In other words, from the fact that the HLB of lecithin is 7 to 9[11)], it is estimated that it is hydrophilic and forms vesicles under the HLB conditions of 9 to 10.

3. Liposome Sensor

Expecting amphipathicity as well as the respective intrinsic specific functions, we tried to construct biomimetic systems by penetrating various kinds of amphipathic molecules into lipidic bimolecular membrane layers of liposomes consisting of phospholipids. It has been reported that nerve excitation causes a morphological change to occur in the spiral structure of the channel protein that exists in the protoplasmic membrane of the nerve fiber through its subjection to a stimulus, and this can be observed with high sensitivity as a delicate change in optical activity.[12)] The author and his group prepared a large monolithic membrane vesicle (LUV, mean grain size of 3.2 μm) by adding a complex of poly-L-lysine (PLL) and octylsulfate (SOS) to L-α-diparmitoylphosphatadyl choline (DPPC) and cholesterol (5:2). We found that PLL has a random structure in proteoliposomic suspension, but that

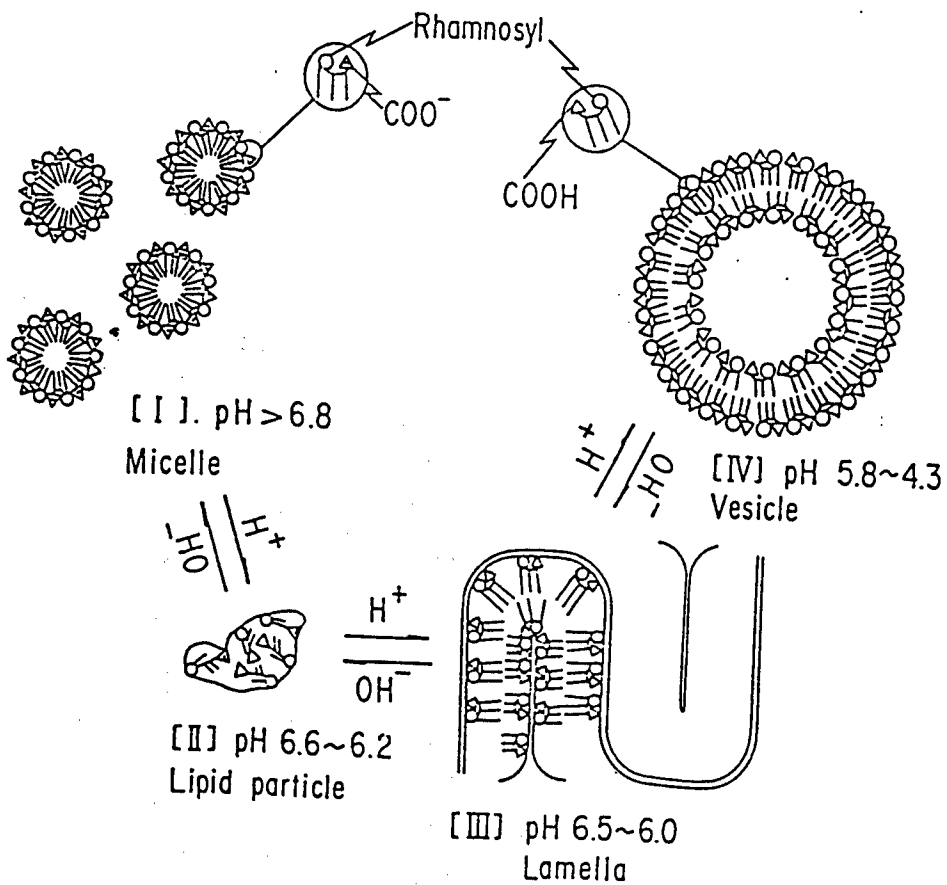

Figure 1. Transformation of Molecular Aggregate of Rhamnolipid pH Dependence

the content of the secondary structure of PLL changes according to the kind of functional group existing in the added substance when an odorant, such as isovalerianic acid that has a short-chained alkyl group (Figure 2), is added.[13] In contrast to the random structure of PLL in the original liposomes, the α-helix content was 30 percent with the addition of isovalerianic acid and the β-sheet content was 15 percent with the addition of methyl isovalerianate, while the α-helix content was 95 percent, the random component 80 percent and the α-helix and β-sheet contents were 10 percent each with the addition of isoamyl alcohol, indicating that the mixtures, as chemical sensors, have detection and identification capabilities. As the principle of identification, one can observe the difference in the adsorption mode due to the hydrophobic or polar reaction to the PLL-SDS complex of the liposomic bimolecular membrane layer. Moreover, with liposomes as the reaction field, we successfully led out the amplified response of chemical stimulation by highly sensitive instrumental analyses (CD spectral and fluorescence and ESR spin probing method). As for the construction of pH response systems, while many projects have been reported, the author's group constructed a molecular system for controlling the release of the inclusion (calceins) in response to pH.[14] When N-palmitoyl-DL-homoserine (PHS) with lactone rings was synthesized and attached to a liposomic bilayer, it was possible to suppress the release of calceins by acidifying the liposomic suspension and to promote the release for pH values exceeding 6.2 or on the alkalinic side. A summary is illustrated in Figure 3. From Figure 4 it is clear that calceins are released when the pH is in the 7.8 to 8.3 range, the release is interrupted when the ambient pH returns to 5.2, and the release and interruption of release are repeated depending upon the pH value. Such a liposome release control function manifests itself in liposomes [yolk phosphatadyl choline, cholesterol and PHS (7:2:1)] that include N-palmitoylhomoserine lactone (PHS). On the other hand, this function was not observed in liposomes carrying dihexadecyl hydrogenphosphate (DCP). As the mechanism for this release control, one can consider the holding of the liposomic wall membrane due to the formation of a lactone ring on the acidic side and the surface activation effect (disturbance or rupture of the bilayer structure) by the amphipathicity on the alkalinic side.[15] This system can be used not only for pH sensors, but also for the pulsed release-type controlled release system desirable for hormonal agents, etc. In a similar manner, we confirmed that, by incorporating amphipathic molecules with redox responsive disulfide bonds in the

bimolecular membrane layer of calcein-incorporating liposomes, and adding ascorbic acid (N,N'-dilauroyl L-cystine, or C_{12}-SS) with reduction properties into the liposome suspension, calceins are released from the central water phase of the liposomes.[16] Further, calcein release was also realizable by using a redox-responsive enzyme *in vivo* which used the proton in glucose as the reducing agent instead of ascorbic acid. As the mechanism for this reaction, it is thought that the two molecules of N-lauroyl L-cystine generated by the reduction of N,N'-dilauroyl L-cystine are surface active and form mixed micelles with the DDPC and cholesterol constituting the liposomic bimolecular membranes, disturbing the membrane structure. The conjectured mechanism is illustrated in Figure 5. The C_{12}-SS content in the liposome wall membrane and the amounts of glucose and enzyme added externally are considered to significantly affect the release rate of the calceins. For example, when 20 μmol of glucose was used for 0.15 μmol of C_{12}-SS, after the slow release of calceins of up to 30 percent within 250 minutes, the calcein release proceeded rapidly, releasing 100 percent of the included calceins in 290 minutes. Therefore, this system forms a signal (in this case, glucose and various enzymes) response type chemical sensor. It should also be noted that the sensing of reducing substances, such as hydrogen disulfide, is also feasible.

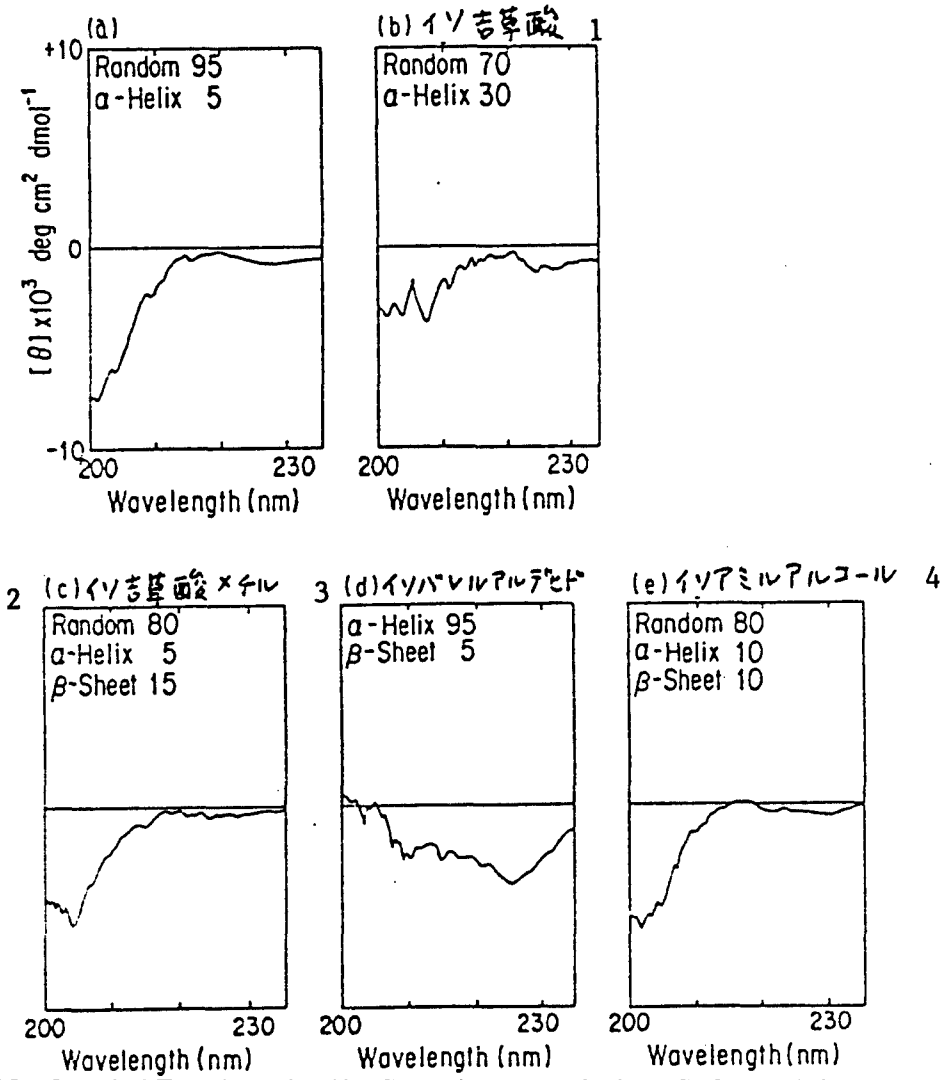

Figure 2. Morphological Transformation (CD Spectra) of Polylysin-Octyl-Sulfate (1:1) Complex Incorporated in Liposome by Chemically Stimulating Substance.[13]

Lipid and polylysin: 6.2 x 10^{-6} mol each; chemically stimulating substance: 1.2 x 10^{-2} parts (V/V) Key: 1. Isovalerianic acid 2. Methyl isovalerianate 3. Isovaleraldehyde 4. Isoamyl alcohol

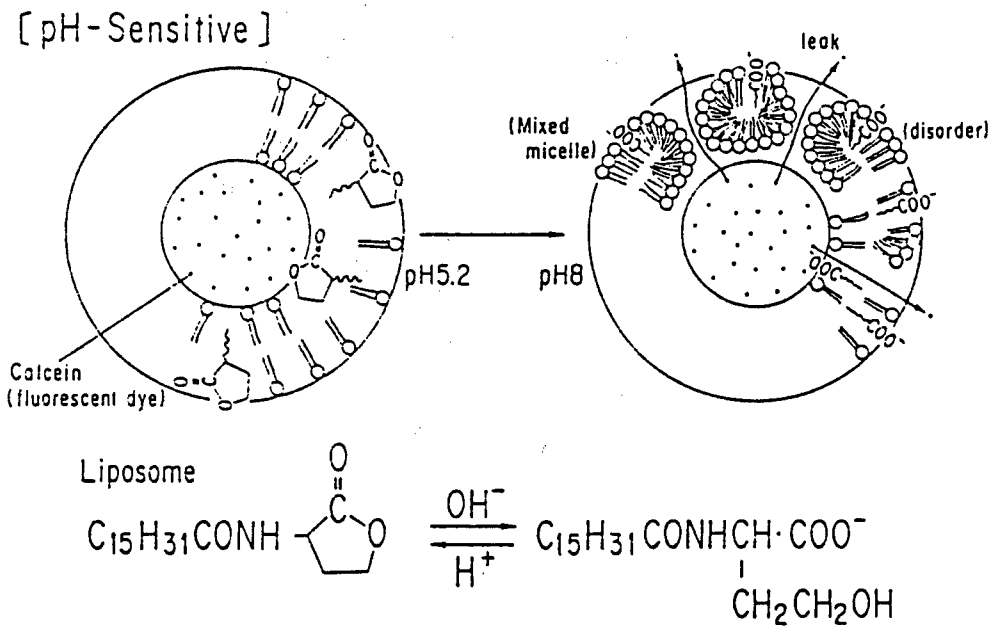

Figure 3. Configuration of pH-Sensitive Liposome (Disturbance of liposomic wall membrane by N-palmitoylhomoserine lactone and release of calceins)[14]

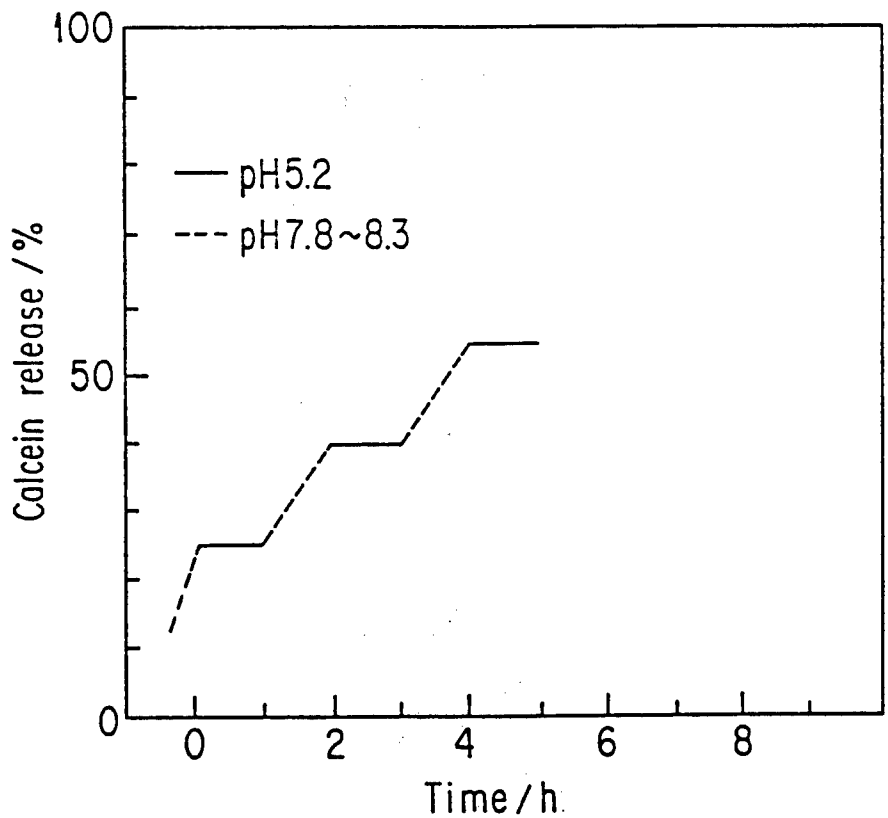

Figure 4. Release Control of Included Calceins via Liposomic Membrane in pH-Sensitive Liposome[14]

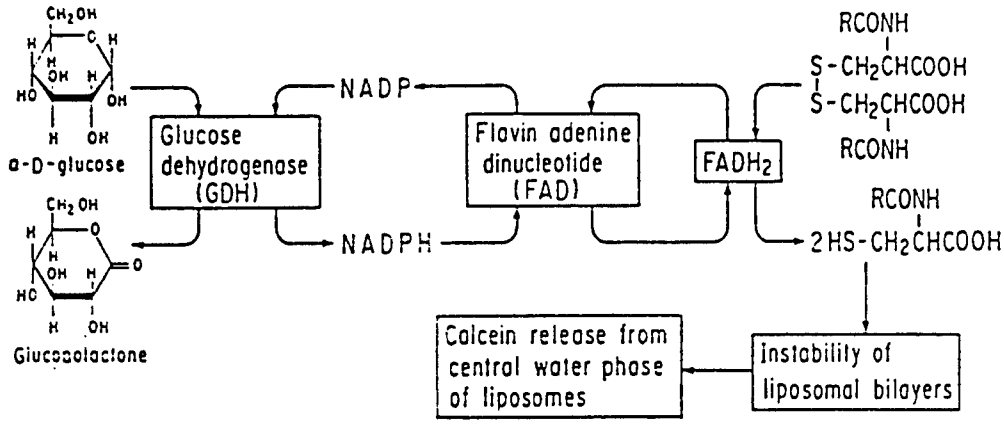

Figure 5. Controlled Release Mechanism of Liposome-Encapsulated Calcein By Means of Glucose-Redox Enzyme to Which Liposome with N,N'-Dilauroyl L-Cystine Embedded in the Wall Layer Has Been Added Externally

4. Chemotaxis of Bacteria and Chemical Sensing[17)-19)]

The chemotaxis of bacteria, i.e., the tendency to move toward food, is considered to represent the prototype of the chemical sensations (taste, olfaction, etc.) of higher animals. For this reason, we tried to compare the response to chemical stimulus substances of bacteria among lower procaryote. Namely, using *Pseudomonas* BOP100 bacteria, which can be assimilated toward glucose and hydrocarbons, we obtaned mature cells by cultivating them for 20 to 40 hours at 30°C while aerating a culture medium consisting of, in addition to 1 percent glucose or 0.1 percent hexadecane as the carbon source, 0.51 percent $NaNO_3$, 0.15 percent KH_2PO_4, 0.15 percent Na_2HPO_4, 0.1 percent $MgSO_4$ x $7H_2O$, 0.01 percent yeast extract (made by DIFCO Labs), 0.001 percent $FeSO_4$ x $7H_2O$, and 0.001 percent $MnSO_4$ x $4.5H_2O$, and used it for the experiment. After trapping 1-pyrenebutyric acid (1-PB) in the cell suspension as the probe, the response to chemical stimuli by butyric acid or methyl butyrate was investigated by measuring the changes in the microsopic polarity (the ratio, F_{378}/F_{398}, of fluorescence intensity for 378 nm to that of 398 nm) in the cellular membrane and the membrane fluidity (E_{448}/F_{398}). The results are shown in Figure 6. The peak shown by the lowermost broken line is the spectrum indicating the spontaneous fluorescence of the culture solution. The lowermost solid curve is the spectrum for the cellular suspension. With the addition of butyric acid, F_{378}/F_{398} decreases, whereas E_{448}/F_{398} increases. On the other hand, with the addition of methyl butyrate, F_{378}/F_{398} hardly changes, although decreasing somewhat with the lapse of time, while E_{448}/F_{398} does not change. When butyric acid is then added, E_{448}/F_{398} increases. When isovalerianic acid or caproic acid is used as a chemical stimulus, a tendency analogous to that of butyric acid is observed. These results agree with the tendency for membrane fluidity to increase when the ESR spin probe method is employed. Next, we reconstructed the membrane components of the cells cultured with hexadecase as the carbon source into lipid microspheres (LMS's), and investigated the response to chemical stimuli using 1-PB as the probe. With the membrane components of the cells and the probe (1-PB), fractions incorporated in the outer layer of LM consisting of phosphatadyl choline similar to vital membrane responds to chemical stimuli. Partial results are shown in Table 1. It can be seen that a response behavior similar to that obtained for living cells, as shown in Figure 6, is exhibited; bacteria respond to the stimuli when butyric acid is added, and they return to the original state with the passage of time. Further, if butyric acid is added after confirming that [the bacteria] has ceased to respond to the methyl butyrate, it responds to it again. In this way, it is shown that the chemical acceptance of LM reconstructed by the fluorescence probe method can be contrasted with the changes in the polarity and fluidity of the vital membrane.

5. Light Transmission and pH Response System by Formation Control of Polyionic Complexes

When polymer ions having different electric charges are mixed in water, a water-insoluble precipitate is obtained. Polyamino acids exhibit similar behaviors, and the results can be related to the formation of secondary structures. Here, we have obtained a system in which the formation of a polyionic complex consisting of poly-lysine and a polyacrylic acid system is made to correspond to the turbidity by controlling the potential.

One-to-one water and ethanol solutions of poly-lysine with various molecular weights (molecular weights of PLL-L 10,000; PLL-H 220,000) and polyacrylic acid (molecular weights of PAA-L 450,000; PAA-H 4,000,000) were mixed at room temperature (25°C), adjusted to a predetermined pH using hydrochloric acid or sodium hydroxide, and the transmissivity (Tr percent) and circular dichroism (CD) of 500 nm light was measured by using a spectrograph (UVIDEC610 made by Japan Spectrograph Co.). Corresponding to the molecular weights and the concentrations of the respective

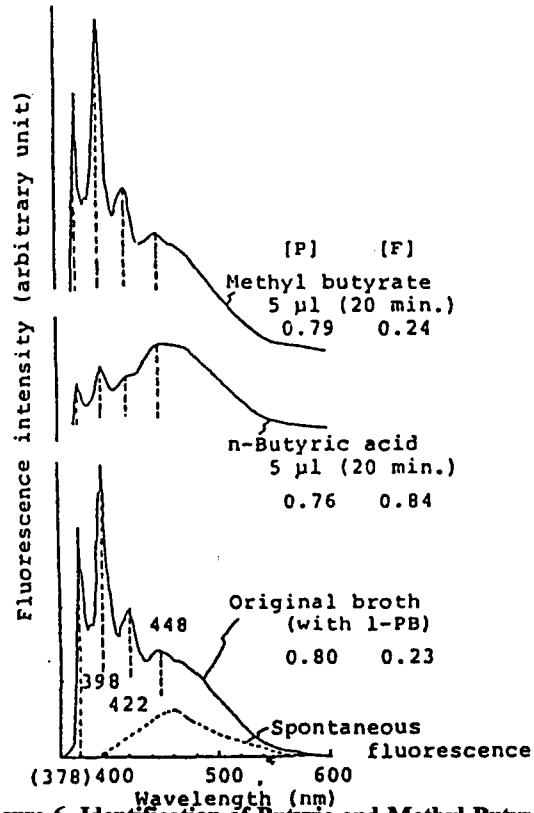

Figure 6. Identification of Butyric and Methyl Butyrate by *Pseudomonas* Cells Grown in Hexadecane

(Probe: 1-PB; excitation light: 350 nm)

polymers and the ratio of mixing of the two, the relationship between Tr and pH exhibited a variety of correlation patterns. It should be mentioned that the values of Tr were smaller, by 4 percent when the difference was the smallest, than the values of the transmissivity

Table 1. Identification of Chemical Stimuli by Lipid Microspheres Obtained by Reconstructing Membrane Components of *Pseudomonas* BOP100 (Probe: 1-PB; excitation light: 350 nm)

	F_{378}/F_{398}	E_{448}/F_{398}
Original LM	1.10	0.12
+n-Butyric acid 5 µl after 20 min.	0.71	0.19
50 min.	0.78	0.28
200 min.	0.92	0.13
+Methyl butyrate 5 µl 20 min.	1.08	0.15
50 min.	1.08	0.11
135 min.	0.97	0.13
+n-butyric acid 5µl 20 min.	0.79	0.12

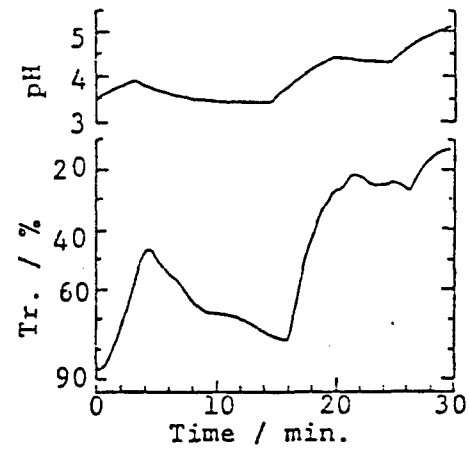

Figure 7. Relationship between pH Adjustment of Polylysine/Polyacrylic Acid Complex System Determined by pH Modulator, and Turbidity of the Solution

(PLL-L: 0.0024 M; PAA-H/PLL-L=0.9; in 0.2 M NaCl Water-EtOH (1:1) solution)

obtained by using an integrating sphere-type hazemeter (NDH-20D made by Nippon Denshoku Co.). We discovered a system which satisfies the appropriate conditions for a polyionic complex, namely, that Tr drops sharply with the pH in the pH range of 3 to 6, that the distributed system of fine particles obtained returns quickly to a transparent solution system with the pH change, and that a quick reversible response between these two states is possible. At this time, the helix content of the system increased along with the pH. Accordingly, it is believed that the helix formation action of the PLL itself is important for a sharp reversible response. When the pH change was controlled using a pH modulator which has a compact ion-selective field effect transistor (ISFET) pH sensor (PH2135 made by Kurare Corp.) built in, in order to demonstrate the relationship between the turbidity of the polyionic complex system thus obtained and the change in the potential, the correspondence pattern between pH and Tr shown in Figure 7 was obtained.

6. Conclusion

Through the biomimetic design of some functions of living beings, it is possible to construct intelligent chemical systems by using diversified biological processes for sustaining living things as the warp and biologically active substances and amphipathetic molecules as the weft. In this report, functional molecules were integrated by employing liposomes, bacteria and polyionic complexes to construct various kinds of chemical sensor systems and controlled release systems which use chemical reactions, pH, hydrophobic and hydrophilic interactions, molecular aggregate forms, diffusion, membrane fluidity or polarity as the control element, verifying the situation in which the functions are manifested.

References

1. Suzuki, K., et al., FRAGRANCE JOURNAL, No 87, 1987 p 60.

2. Wendel, A., Ghyczy, M., SOAP/COSMETICS/ CHEMICAL SPECIALTIES, June 1990 p 32.

3. Hayward, J.A., Smith, W.P., COSMETICS AND TOILETRIES, Vol 105, July 1990 p 47.

4. Osawa, F., et al., ed., "Structure of Functional Elements," Chapter 4 (by Akuzu and Kyogoku), Asakura Shoten, 1976.

5. Nozawa, Y., PHARMACIA, Vol 22, 1986 p 1363.

6. Kayama, M., ed., "General Lipid Chemistry," 11-3 (by Ishigami), Koseisha-Koseikaku, 1989.

7. Ishigami, Y., et al., CHEM LETT, 1987 p 763.

8. Ishigami, Y., et al., PETROLEUM CHEMISTRY, Vol 36, 1987 p 490.

9. Ishigami, Y., Machida, H., J AM OIL CHEM SOC, Vol 66, 1989 p 599.

10. Israelachvili, J.N., et al., QUAT REV BIOPHYS, Vol 13, 1980 p 121; Asano, et al., ed., "Supplement 101 to Chemistry, Recognition and Response of Cells and Membranes," Chapter 4 (by Yamada), Kagaku Dojin Publishers, 1983.

11. Yamano, Y., PETROLEUM CHEMISTRY, Vol 35, 1986 p 478.

12. Watanabe, A., MEMBRANES, Vol 12, 1987 p 118.

13. Ishigami, Y., BIOCHEM INTERN, Vol 19, 1989 p 777.

14. Okabe, H., et al., MEETING OF CHEMICAL SOCIETY OF JAPAN, 1990 p 1054.

15. Isomaa, B., ECOLOGICAL BULL, Vol 36, 1984 p 26.

16. Okabe, H., et al., CHEM EXPRESS, Vol 6, 1991 p 315.

17. Ishigami, Y., et al., PAPERS FOR 22ND SYMPOSIUM ON TASTE AND SMELL, 1988 p 217.

18. Ishigami, Y., et al., PAPERS FOR 23RD SYMPOSIUM ON TASTE AND SMELL, 1989 p 209.

19. Ishigami, Y., et al., PAPERS FOR 24TH SYMPOSIUM ON TASTE AND SMELL, 1990 p 251.

20. Sawai, T., et al., J ELECTROANAL CHEM, in press.

NTIS
ATTN PROCESS 103

5285 PORT ROYAL RD
SPRINGFIELD VA 22161

Foreign Broadcast Information Service (FBIS) and Joint Publications Research Service (JPRS) publications contain political, military, economic, environmental, and sociological news, commentary, and other information, as well as scientific and technical data and reports. All information has been obtained from foreign radio and television broadcasts, news agency transmissions, newspapers, books, and periodicals. Items generally are processed from the first or best available sources. It should not be inferred that they have been disseminated only in the medium, in the language, or to the area indicated. Items from foreign language sources are translated; those from English-language sources are transcribed. Except for excluding certain diacritics, FBIS renders personal names and place-names in accordance with the romanization systems approved for U.S. Government publications by the U.S. Board of Geographic Names.

Headlines, editorial reports, and material enclosed in brackets [ ] are supplied by FBIS/JPRS. Processing indicators such as [Text] or [Excerpts] in the first line of each item indicate how the information was processed from the original. Unfamiliar names rendered phonetically are enclosed in parentheses. Words or names preceded by a question mark and enclosed in parentheses were not clear from the original source but have been supplied as appropriate to the context. Other unattributed parenthetical notes within the body of an item originate with the source. Times within items are as given by the source. Passages in boldface or italics are as published.

SUBSCRIPTION/PROCUREMENT INFORMATION

The FBIS DAILY REPORT contains current news and information and is published Monday through Friday in eight volumes: China, East Europe, Central Eurasia, East Asia, Near East & South Asia, Sub-Saharan Africa, Latin America, and West Europe. Supplements to the DAILY REPORTs may also be available periodically and will be distributed to regular DAILY REPORT subscribers. JPRS publications, which include approximately 50 regional, worldwide, and topical reports, generally contain less time-sensitive information and are published periodically.

Current DAILY REPORTs and JPRS publications are listed in *Government Reports Announcements* issued semimonthly by the National Technical Information Service (NTIS), 5285 Port Royal Road, Springfield, Virginia 22161 and the *Monthly Catalog of U.S. Government Publications* issued by the Superintendent of Documents, U.S. Government Printing Office, Washington, D.C. 20402.

The public may subscribe to either hardcover or microfiche versions of the DAILY REPORTs and JPRS publications through NTIS at the above address or by calling (703) 487-4630. Subscription rates will be provided by NTIS upon request. Subscriptions are available outside the United States from NTIS or appointed foreign dealers. New subscribers should expect a 30-day delay in receipt of the first issue.

U.S. Government offices may obtain subscriptions to the DAILY REPORTs or JPRS publications (hardcover or microfiche) at no charge through their sponsoring organizations. For additional information or assistance, call FBIS, (202) 338-6735,or write to P.O. Box 2604, Washington, D.C. 20013. Department of Defense consumers are required to submit requests through appropriate command validation channels to DIA, RTS-2C, Washington, D.C. 20301. (Telephone: (202) 373-3771, Autovon: 243-3771.)

Back issues or single copies of the DAILY REPORTs and JPRS publications are not available. Both the DAILY REPORTs and the JPRS publications are on file for public reference at the Library of Congress and at many Federal Depository Libraries. Reference copies may also be seen at many public and university libraries throughout the United States.